Franky Kumar Kalia[1], Dr Kalyan Kumar Das[2*]

Investigation of Inner and Outer Flow Field Characteristics of Pyramidal Roof Rectangular Base Building Due to Synoptic Wind Flow through it by Changing the Wall Porosity of the Building.

Journal of Electrical Systems

ABSTRACT: A key component of building design involves understanding the flow field that develops near a building due to synoptic wind flow across it. The wind environment around buildings is important for their structural strength, but it also has an impact on ventilation effectiveness, pedestrian comfort, and the spread of pollutants. Modern structures now have a variety of apertures, including windows, doors, and ventilators, leading to the rise of the green building idea and environmentally friendly living. The flow field becomes more complex as a result of these apertures, which alter the flow properties inside and outside the building. The goal of the current study is to better understand the flow fields surrounding the structures with openings, both internally and externally. This study aims to examine the wind flow over structures with Pyramidal roof rectangular base building that have openings exposed to synoptic winds. Using the Computational Fluid Dynamics (CFD) approach, internal flow within the buildings is also examined for optimal ventilation. Numerical simulations are conducted using ANSYS-FLUENT, a commercially available CFD program. The steady Reynolds Averaged Navier Stokes (RANS) equations are solved by numerical simulations. This study examines the effects of various wall porosities on the building façade as well as the relative vertical placements of the openings. The flow field both within and outside of buildings is significantly impacted by wall porosities and the relative vertical positions of openings on building facades. The internal pressure distribution and air flow rate are greatly influenced by the wall porosity. The study provides information about the flow environment within and outside of a low-rise building with Pyramidal roof rectangular base building with openings, which is useful for estimating wind loads for the building's structural design and for creating a natural ventilation system.

Keywords: ventilation, estimating, Pyramidal, CFD, environment

1. INTRODUCTION

A difference in air pressure causes air to move, which is known as wind. Although wind can be utilized to generate electricity, it can also cause destruction when it causes storms, cyclones, and other natural disasters. Wind loads the buildings and other structures that stand in its route. With the right design, this building can withstand the damage caused by wind, protecting both life and property. In general, wind is turbulent, and when it hits buildings or other objects, the turbulence becomes more complex. As a result, predicting the flow characteristics that the wind produces around these things becomes more difficult. Buildings are one of the most crucial components of both urban and rural environments, and their number is growing daily as the population rises. Because of phenomena including flow separation, reattachment, and vortex generation, the flow field surrounding the building is extremely complicated. When wind hits a building, it applies pressure to the roof and walls, imposing aerodynamic load on the building's structure.Accurate estimation of the wind-induced load is necessary for a building's safety. The foundation for calculating wind load is the distribution of pressure and velocity around the building. Understanding the pressure and velocity field surrounding the building is crucial. The ventilation effect is the process by which wind enters a building through apertures and exits through other openings due to pressure differences. Therefore, when it comes to efficient natural ventilation, a building's pressure distribution is crucial. The pollutants created by indoor pollutants, automobile exhaust, and other external contaminants should be eliminated from the buildings in order to maintain a healthy interior atmosphere. Understanding the flow field both inside and outside makes it easier to drive out contaminants. People may find it challenging to walk due to the horseshoe-shaped vortex that developed near the base of the building and the corner streams. Therefore, it is crucial to understand the velocity field near the building. It is clear from the discussion above that the problem of wind flow over buildings has drawn attention from academics for many years due to its complexity and variety of real-world uses. The two primary forms of ventilation systems found in buildings are mechanical and natural ventilation. Mechanical ventilation systems, which use mechanical power, are one source of greenhouse gas emissions. In addition, it has been noted that poor mechanical ventilation system design and maintenance are the main causes of a number of health issues, such as sick building syndrome (SBS) [45]. Conversely, natural ventilation doesn't need energy. The air

[1] Phd Research Scholar Energy Engineering Department, Assam Science and Technology University (Assam), Email Id: frankykalia1234@gmail.com
[2]*Professor, Mechanical Engineering Department, Assam Engineering College(Assam), Email Id: kkdas1971@gmail.com

flows through the inhabited space of the building due to the pressure gradient created by the wind. Therefore, natural ventilation is an effective ventilation system to maintain thermal comfort and a healthy interior environment. It is also cost-effective and environmentally beneficial. There are apertures on several building faces that allow for natural ventilation. One of the most crucial elements of the building's geometry is its apertures, which affect the flow fields both inside and outside. Openings are necessary in buildings for natural ventilation. The building façade's apertures alter the flow fields inside and outside. With the rise of the idea of green buildings, natural ventilation systems have become an attractive option for designers to investigate because variations in the flow field affect both the ventilation process and the wind load exerted on the building's surface. A thorough analysis of the interior and exterior flow fields generated by wind in a building is necessary to improve natural ventilation and create a stable structure. Wind flow over structures with openings is an issue of great practical importance, which is what inspired us to conduct this work. Computational fluid dynamics (CFD) is a subfield of fluid mechanics that solves fluid flow-related problems through numerical analysis.

CFD is gaining popularity due to its capacity to numerically analyse and visualize the flow around complexly geometrized structures. Consequently, wind engineering makes extensive use of it. In addition, it is less expensive and time-consuming than wind tunnel testing and full-scale measurement methods. When compared to numerical analysis, full scale measurement and wind tunnel testing are more difficult, time-consuming, and expensive procedures; however, they cannot be disregarded because they are necessary to validate the CFD code and guarantee that the results of the CFD simulation are satisfactory. The wind-induced flow fields inside and outside of a structure with openings are influenced by a variety of elements. Opening sizes, building geometry, wind directions, and opening placements all affect the pressure and velocity distributions inside and outside the structure. Having a better understanding of the flow field's characteristics can help to improve structural integrity and accurately predict the loads acting on the structure. Additionally, it makes it easier to plan and construct an efficient natural ventilation system. The impact of the aforementioned factors on flow fields is examined numerically in this thesis. The numerical calculations are carried out using the CFD software ANSYS-FLUENT Version 2020 R1. The stable Reynolds Averaged Navier Stokes (RANS) equation has been solved using the k-Ω turbulence model of Shear Stress Transport (SST).

2. LITERATURE REVIEW

Through the 1970s, it was noted shortage of fossil fuel, which was a global issue and decreasing the energy consumption rate came across as one measure. Thus, it is natural that under such conditions achieving a thermally comfortable and healthy indoor environment with no energy input would be alternate. This mandated significant investigations into the phenomena of natural ventilation.

An overview of the various literature works on wind flows past buildings with openings is provided in this section. The majority of research on wind flow around structures with openings focuses on natural ventilation.

If a turbulent impinging jet hit an enclosure with a single opening, a complicated mechanism of interplay between various effects causes the air to exchange across the aperture due to varying exterior air velocity. After conducting an experimental investigation, Cockroft and Robertson (1976) [1] developed a basic model that made it possible to link ventilation to external air flow. Up until that point, it was impossible to estimate air flow, infiltration, and natural ventilation in structures with any degree of accuracy. This investigation clearly showed how much airflow was ventilated by turbulent wind. Since the process is more intricate, more theoretical and experimental research was recommended.

Chu et al. (2015)[2] have investigated experimentally the Natural Ventilation on One Side of a Building Having Two Openings on the Same Wall Using the tracer gas approach, the effects of wind speed, wind direction, and opening living area on the air exchange rate . The air exchange rate was higher with two openings than with a single opening, according to the results. Additionally, greater exchange rates were attained for wind directions between 22.5 and 67.5 degrees, and a phenomenon known as shear ventilation was noted when the angle between the opening orientation and the direction of the incident air was zero degrees or parallel, in this case a very little amount of impact on the ventilation is seen due to location of the opening. One of the factors examined in this paper was the impact of internal partitions on ventilation, which was also looked into. As a result of the internal split, the exchange rate of wind decreased. In the event that a building has internal partitions is unaffected by wind speed and opening area. When a semi-empirical model was compared to experimental data, a small amount of inaccuracy was observed. The model used the time average pressure drop and pressure fluctuation to predict the exchange rate.

The single-sided natural ventilation studies are highly challenging due to number of internal and external factors interrelated with it. There was no appropriate tool to predict air flow rate through a single opening in buildings. Characterizing single-sided natural ventilation experimentally, Dascalaki et-al (1996)[3] compared with the flow network model existing at that time. In Passys Test Cell in Athens, Greece full scale experiments was conducted. The airflow rate through the opening was measured using the tracer gas technique. Wind speed of the wind was actually measured using laboratory hot wire anemometers and commercial sensors. Additionally, PASSPORT-AIR, a computational tool for network modelling based on Bernoulli's Theorem, was used to compare the experimental result. Difference in Air Velocity Between Measured and Predicted Network flow models are unable to account for the effects of turbulence near or around the entrance. The vertical profile of the wind velocity at the opening changes from its entrance depending on its horizontal position which indicates more measurement need to be carried out. As a result, extra parameters along the opening's width are required. A new coefficient, k, has been proposed, which is defined as the ratio of air flow rate based on the vertical profile of the wind velocity in the middle of the opening to the actual air velocity calculated by the tracer gas experimental results. It is seen that the coefficient k is inversely proportional to the temperature difference. The complete effect of wind speed in this work could not be determined, since the flow direction was parallel or behind the opening. Still, this research gives a better indication in the process of single-side natural ventilation.

Eftekhari (1995) [4] conducted research on the effects of external wind speed and direction on thermal comfort and air flow patterns in a naturally ventilated office building. Three windows on one side of the climatic chamber served as the site of the experiments. Temperatures and air velocity in the environmental chamber were recorded during the single-sided ventilation. The comfort analysis inside the environmental chamber was done by parameters PPD (Predicted Percentage of Dissatisfaction) and PMV (Predicted Mean Vote) averages . In conclusion The study's outcomes have emphasized how important it is to take window heights and solar shading effects into account when designing natural ventilation for thermal comfort. The indoor air velocity, PPD and PMV values were influenced by the outside wind velocity..

A door or window failure in the face of high winds can produce extremely large internal pressures. for application of quasi-steady theory to determine peak external and peak internal pressures on sealed buildings and with opening Ginger & Letchford, (1999)[5] has conducted multiple experiments at Wind Engineering Research Field Laboratory (WERFL) at Texas Tech University. The results of these tests demonstrated that an opening in a likely windward wall dominant decreased positive loads on the windward wall and higher negative loads on roof, sidewalls, and leeward wall compared to a nominally sealed building; The peak net pressures on some parts (i.e. the roof windward edge) of the building with a dominant windward wall opening were smaller than the measured values. The net peak suction pressure at the roof windward edge region which experiences large suction pressures was 93% of the peak external-peak internal value, which indicates that the large positive internal pressures and the large suction roof windward edge pressures were well correlated.

Guha et al (2011)[6] investigated various factors such as effect of opening size, effect of background leakage that impact the internal pressure fluctuation due to dominant single sided openings in a low rise building. Guha et al (2012)[7] has done a theoretical and wind tunnel research and compared with the most crucial single opening scenario to examine the interior pressure dynamics of a building with several opening on a single wall and highly correlated exterior pressures. The findings show that when the ratio of opening sizes increases, internal pressure fluctuations in these configurations also increase and eventually approach the value of the most critical single opening configuration when the total area of the two openings doubles the critical single opening size. Both mean flow component and fluctuating flow component [8] play a important role in investigating ventilation flow. Most studies considerd only mean pressure distribution and mean velocity to examine natural ventilation only few studies [9,10,11] have considered fluctuating components of flow parameters for investigating natural ventilation cases

Turbulence is the major consideration in case of single-sided wind-driven natural ventilation, hence it makes it extremely difficult to predict this type of flow. The use of Computational Fluid Dynamics (CFD) offers another way to study the flow at a specific point inside and in proximity to building. Jiang et al (2003)[12] has examined three different cases of air flow in and outside a building using LES (Large Eddy Simulation) SS model. In their work, a opening is first situated at the windward wall then in leeward and on both leeward and windward wall for studying cross-ventilation flow of air. The output of numerical simulation is in a good agreement with the results from wind tunnel experiment. They found that LES is a suitable technique for mathematically determining the single-sided ventilation flow.

Kato et al(2006)[13] used a indirect technique to increase the air flow rate through a single sided opening because air flow rate from single sided opening is much lower than a two sided opening. He carried wind tunnel experiments and exchange of

air was measured using a constant injection tracer gas technique. Some vanes were attached to the openings whose vertical axis were aligned with the centre of windows to increase the air flow rate. In some cases for weaker natural flow circulation was induced by rotating the vanes at 2rev/sec. the overall result shows that attachment of vanes in a single sided opening increases the ventilation efficiency.

In the case of both single-sided and cross ventilation phenomena, the velocity of airflow through the aperture was typically estimated using the orifice equation, which was based on Bernoulli's theorem. The major gap in these calculations was taking coefficient of discharge (Cd) as constant which was questioned by Heiselberg et al. (2001)[14]. After carrying out a number of tests, they discovered that coefficient of discharge varies depending on the kind of window and the opening area.

Larsen and Heiselberg [23] found that all previous methods used to estimate the ventilation rate in single-sided natural ventilation had completely neglected the effect of the wind incidence angle. Meanwhile, wind angle of incidence has a significant effect on the two major driving forces of natural ventilation, ie temperature difference and wind pressure. Therefore, they suggested a novel design expression for determining the ventilation rate as a function of wind incidence angle based on the series of wind tunnel studies.

Karava et al (2005)[24] had done multiple experiments in Boundary Layer Wind Tunnel on a building with openings on different walls (cross ventilation) to investigated how opening area and inlet to outlet ratio impacts the internal pressure coefficients and discharge coefficients of a building having facades of cross ventilation. They find that in buildings with unequal inlet and outlet opening, pressure coefficient varies considerably. They also finds that inlet discharge coefficient changes with the opening area and inlet to outlet ratio. Moreover, they had not considered impermeable models (models without leakage) and considered background leakage of 0.5% in their model. Thus, their study result has a limitation of use.

CFD was used as an excellent tool against experimental work because of its accuracy by Meroney(2009)[25], cross ventilation's code fluent was used for Numerical simulation to replicate the result obtained from boundary layer wind tunnel tests which was done by Karava (2008)[26]. He tested his work in RANS based turbulence models viz. Standard k-ε, Realizable k-ε, RNG k-ε, k-ω, and RMS model in addition to Direct eddy simulation (DES) and LES turbulence models. The turbulence models he had considered can predict the flow characteristics with satisfactory accuracy however slight variations were seen in case of the above models. Although the various turbulence models have an impact on the exterior flow, the interior flow has shown very little variance. This work convinced and restore the Researcher belief to use CFD as a tool for natural ventilation analysis for future work.

Karava et al. (2011)[27] find a relationship between internal airflow patterns with the design and placement of openings on the cross-ventilation building. They conducted an advance experimental test based on particle image velocimetry (PIV) at the wind tunnel. In their study they find that internal pressure distribution and induced airflow rate is notably impacted by the internal airflow patterns moreover relative inlet outlet position and inlet-outlet ratio are important parameters including porosity of wall for the assessments of airflow in the cubic type buildings.

In order to study the wind-induced cross-ventilation in a building, Katayama et al. (1992)[28] conducted both wind tunnel tests and full scale measurements. Afterwards, Iino et al. (1998)[29] examined the air flow characteristics in five distinct building models as a result of air-driven cross-ventilation using both numerical simulations and wind tunnel measurements. Ohba et al. (2001)[30] and True (2003)[31] also examined the interior and external flow parameters in a cross-ventilated building.

Large eddy simulation (LES) model was used by Chu and Chiang (2014)[32] to investigate how flow rate of building is influenced by building length in cross ventilation. They first validate their simulation result with wind tunnel experiments and then create a model that is predictive to estimate the resistance factor and ventilation rate in long structures. Their Studies result had demonstrated that aspect ratio L/H has a greater influence of pressure on leeward side than windward side and that the rate of ventilation of short buildings would be higher compared to the case of long buildings because of internal resistance for the same pressure difference. In this study internal resistance was taken in to account which was ignored by the traditional ventilation models which causes the ventilation rate to be exaggerated in traditional ventilation models. This study also demonstrated how the ventilation mechanism is impacted by the opening location. According to the result of above study building with opening on the opposite corners of the windward and leeward side had 15.5% lower rate of ventilation than building with opening in the centreline.

The effectiveness of steady RANS and LES turbulence models in determining the cross-ventilation flow in a enclosure was assessed by van Hooff et al. (2017)[33]. They used five distinct turbulence models in RANS simulations namely 1)Reynolds Stress Model (RSM), 2) Standard k-epsilon model 3) RNG k-epsilon model 4)RLZ k-epsilon model and 5) SST k-omega model and dynamic Smagorinsky subgrid-scale (SS) model in LES . The mean velocity, turbulent kinetic energy, ventilation flow rate, incoming jet angle, and incoming jet spreading width are the parameters that have been chosen for assessment. They experimentally observed jet's direction correlates with the SST k-omega, RNG k-epsilon, and RSM models. They underscore the drawback of stable RANS models which cannot catch the higher value of turbulent kinetic energy and only lower values of turbulent kinetic energy were seen above and below the jet which shows the inability of RANS models' to accurately replicate turbulent kinetic energy. Their findings explains why the steady RANS models are unable to describe the jet's vertical flapping. Their results shows that LES reproduces the flow's transient behavior more accurately than RANS models, it can more accurately estimate the flow's parameters such as velocity, turbulent kinetic energy, and volume flow rate. They stated that the target parameter (no of grids, turbulent kinetic emery) should be taken into consideration while choosing the turbulence model. They also pointed out that LES needs a higher grid resolution, which considerably raises the computing cost.

Manolesas et al (2018)[34] experimentally explored the wind flow parameters around a cubic building which has verical opening on opposite facades and compared the flow parameters with an identical building model. Two distinct upstream conditions 1) High Shear, 2) Low Shear were taken into consideration in order to examine the impact of upstream boundary layer conditions. They found that estimated pressure of the surface model matches the results of the benchmark measurement. In their investigation they found that both the pressure field and velocity in the area around the building are significantly impacted by both the upstream boundary conditions and ventilation rate. The rate of ventilation calculated from the velocity profile near the openings and the rate of ventilation calculated from the orifice equation were also compared and they found that in orifice equation both rate of ventilation and the impact of upstream boundary conditions get overstates(larger).

Zhang et al (2020)[35] conducted, a comprehensive comparison of cross-ventilation and single-sided ventilation within a cubic structure with a large number of wind incident angles. The effectiveness of the RANS and LES models in predicting natural ventilation was also assessed in the current study. Although LES model is better than RANS models in terms of performance, but it is not cost effective. The tracer-gas decay method and the integration of the opening velocities approach were the two techniques used to estimate the ventilation rates. They observed that more accurate results are produced when the LES model is paired with the tracer-gas decay method.

While a lot of research has been done on cross-ventilation, isolated structures have received the majority of attention. Research on cross-ventilation in densely populated urban buildings was lacking. Square and staggered building arrangements were the two types of building arrangements that Chiyoko et al. (2022)[36] examined.Tong et al. (2016)[37] and Bady et al. (2011)[38] made an effort to deal with this problem. Shirzadi et al. (2019)[39] and Shirzadi et al. (2020)[40] subsequently examined the cross-ventilation flow across a building in a densely populated metropolitan area. They investigated the cross-ventilation of the target building which was affected by different wind directions and metropolitan environments ranging from moderately to densely populated. The findings showed that the channelling effect created by the nearby buildings has a notable influence on the airflow pattern both within and outside the target building. Cross ventilation becomes sporadic (changes frequently) in character in highly dense environment.

Zhang et al. (2022)[52] investigated the impact of various external and internal opening configurations on cross-ventilation in a generic building using computational fluid dynamics (CFD) simulations. The effectiveness of ventilation rate for two opening configuration in a cross ventilation increases according to their simulation results. According to their study for windows of equal size rate of ventilation of two opening configuration is twice that of single opening configuration. According to their study, ventilation rates are always reduced by internal walls and a linear reduction is seen with the internal blockage ratio.

Kobayashi et al. (2022)[53] uses LES model to investigate wind induced natural building in an isolated building. Their study aims to differentiate between two approaches used to estimate the ventilation rate: 1) Bulk airflow rate (AFR) and2) Purging rate (PFR), also known as purge flow rate and finds that ventilation effectiveness is the ratio of PFR:AFR. According to reports, the ventilation effectiveness values are 70–80% for the double-sided apertures, 60%, for single-sided openings on the lateral side and 90%, for windward and leeward sides. The study also recommended that two important phenomena, pulsing flow and eddy penetration, must be considered for the estimate of AFR.

Díaz-Calderón et al.(2023)[54] investigated cross-ventilation in an isolated building with symmetric opening positions using CFD models. To examine the impact of opening placements, openings are positioned at the top, middle, and bottom of the building's facades

On inlet and outlet surface respectively.By changing the aperture height, the impact of wall porosity was also investigated. The study discovered that the most effective ventilation performance is achieved by designs with middle and bottom openings with 0.2 wall porosity.The limitation in their study is that they have used simple cubic building with flat roof but building roof shape is a important factor in calculating natural ventilation flow rate as it affects the surrounding flow field [25][55]. Therefore several other researcher had considered roof shape such as curved roof, gable roof pyramid roof to investigated natural ventilation phenomenon.

Gable roof designs are the most typical for low-rise buildings. In light of this, numerous researchers have looked into natural ventilation in gable roof structures [56, 57]. The effect of internal pressure on crossventilation was examined by Karava et al. (2006)[58]. They study at a gable roof building model with openings on the side and windward walls. They finds that internal pressure is influenced by wall porosity and the ratio of inlet to outflow, which in turn impacts the indoor airflow pattern.

Yi et al. (2018) [59] investigated the airflow characteristics within a naturally ventilated dairy fire using wind tunnel tests utilizing a scaled model. This work's main goal is to determine how the size and positions of sidewall openings affect the interior ventilation field in an animal-occupied zone (AOZ). 2D Laser Doppler Anemometers (LDA) were used to measure the velocity within and outside the building model. When the opening ratio was less than 62.71 percent and the apertures were placed below the eaves, the indoor flow field is characterized by an "up jet" flow. When sidewalls were absent, air moved through the AOZ without interacting with the surrounding atmosphere. The researchers also discovered that there is a far more complex relationship between the opening size and the turbulence intensity Where there are high-side walls in the AOZ, homogenous air speed distributions are seen. On the other hand, when there was no sidewall at the bottom of the AOZ, airflow heterogeneity became visible. A number of further studies [60], [61], [62], [63], [64], and [65] also looked into cross-ventilation in gable roof structures with roof and side wall apertures.

The wind-induced flow field surrounding an isolated gable-roof house with and without openings was studied by Xing et al. (2018a) [66]. The impact of opening position and wind direction on the pressure distribution surrounding the building was examined using numerical models. The findings of the numerical computation are compared with the measurements made in the wind tunnel. Four distinct building configurations were examined for the pressure distribution namely 1) Enclosed, 2) One windward opening, 3) One windward opening and One side wall opening and 4) One windward and two side wall openings. The combined action of both external and internal pressure causes the roof to experience a higher net pressure with the opening on the windward wall. This observation is consistent with research work of Sharma and Richards. (2005) [67]. This net pressure reduces significantly when there is opening on the side walls. They also observed that suction appears on the upwind roof corner near the windward walls when wind incidence angle become oblique. They find that as the wind incidence angle increases, the internal pressure coefficient falls.

The act of opening windows and doors to increase natural ventilation is known as "airing." To remove contaminated air indoors, airing out is crucial. The majority of earlier research focused mostly on ventilation through windows. However, ventilation through doors is essential in huge structures like churches and museums. Thus, in a structure with a gable roof, Kobayashi et al. (2010) [68] researched into cross ventilation through doors. CFD simulations and wind tunnel tests were both carried out by them. The sand erosion approach was used to visualize the interior flow. The study additionally explored at the impact of different opening sizes. After that, Hayati et al. (2018) [69] used a wind tunnel to conduct an experimental study on airing generated by wind flow through door openings. For the study, an extended building model with entrances in the center of the long side of the building was taken in to consideration and both single and cross ventilation flow was examined. The tracer gas approach was used to evaluate the air change rate. Airing rate is increased by 4 to 20 times in cross flow airing when compared to single opening airing. Additionally, when doors are positioned at the windward wall airing is 53% higher when compared to the doors present in leeward wall in the case of single-opening airing. Additionally, study on the airing rate of a draught lobby (extended entrance space function like wind lock) was investigated and found that airing rate is reduced by 27% and turbulence level increased by 38%.

Esfeh et al. (2021) [70] investigated natural ventilation in an isolated room model with a semi-circular roof using both experimental and numerical methods. For the current study, a scale model of a single cubic structure with a semi-cylindrical roof and two openings viz 1) One at the roof and 2) One at the windward surface is taken into consideration. To determine

the discharge coefficient of the building opening pressure and velocity field inside the building were measured. The findings showed that a curved roof structure's ability of natural ventilation is highly dependent on the direction of the wind.further curved roof height is an important factor for increase recirculation flow with in the building. The results show that the direction of the wind has a significant impact on a curved roof structure's capacity for natural ventilation.

The wind-driven cross-ventilation flow in a typical isolated low-rise building with a sawtooth roof was examined by Perén et al. (2015)[71]. The coupled approach of CFD simulation was used in the computational domain using the coupled approachThey examined how the flow characteristics were affected by the angle of the roof's inclination and the outlet opening's vertical location. The findings showed that the volume flow rate and indoor air flow pattern are significantly impacted by the roof inclination angle.

The ventilation performance of buildings with single-span and double-span sawtooth roofs was examined by Perén et al. (2016)[72]. They tested different structure of roof configurations, including concave, convex, and straight roofs. Additionally, the effect of the ratio of input to output opening was examined. The ratio of the inlet opening area to the sum of total outlet opening areas was defined as the opening ratio. Using the SST k-ω turbulence model, the 3D stable RANS equations were solved. From the CFD simulation results, it was shown that the convex kind of roof layout had the largest volume flow rate for both single- and double-span leeward sawtooth roofs. Furthermore, it was shown that double-span roofs performed better for straight and concave roof geometries than for single-span roofs. Regardless of roof geometries, the volume flow rate rises noticeably with an opening ratio of less than 1. The limitation in this work is that this study was carried out for one incidence angle normal to the opening.

Singh and Roy (2019)[73]have numerically investigated the Pressure distribution on the Pyramidal roof building of Pentagonal and Hexagonal Plan- low-rise building using CFD. A Reliazable K-ε model was used for numerical simulation. Five models of Pentagonal base and five models of hexagonal base Pyramidal building with roof Roof angle of ⟦20⟧^°,⟦25⟧^°,⟦30⟧^°,⟦35⟧^° & ⟦40⟧^°were tested by them with wind direction 0^°,⟦15⟧^°,⟦30⟧^° & ⟦45⟧^°. In their study they found that as the roof slope increases, negative pressure coefficient or suction increases while roof slop does not effect much the positive pressure coefficient of both type of buildings. For all roof slopes, the area closest to the ridge line between the windward and leeward faces of the roof surface had the greatest negative pressure or suction. Neither in Indian standard of wind load nor in European standard pressure coefficient value of Pyramidal roof is absent therefore they compared their result with the pressure coefficient of hip-roof. Based on the pressure coefficient values and other roof parameters provided in both wind standards, the area-weighted average values are calculated [74,75]. By comparing they found that Pyramidal building with hexagonal plan and Pentagonal plan are better than hip roof building. Finally, they found that the hexagonal pyramidal roof surface building was shown to have higher pressure coefficients in the roof than the pentagonal pyramidal roof surface building therefore its longevity increases. This may be because of the better wind distribution throughout the roof surface by hexagonal pyramidal roof surface building.

3. COMPUTATIONAL DOMAIN

The model under consideration in this study is a pyramid-roofed rectangular building with dimensions of 20 m in length, 8 m in width, and 6 m in eaves height (H), as illustrated in figure 3.1. The model has two comparable rectangular openings of dimension (l x h) m2 on the windward and leeward sides. The dimensions of the computational domain are based on research by Singh and Roy (2019) [78] and Revuz et al. (2012) [77].Upstream length, vertical height, and side-wall width are all 5H, measured from the building's side walls, roof, and windward wall, respectively. Figure 3.2 illustrates the downstream length, which is 15H measured from the building's lee walls. Lastly, (128m x 80m x 36m) is the domain's size.

3.1 Geometry: In ANSYS Fluent, geometry is created as per the dimension given above.

3.2 Meshing: After creating geometry, this is the next crucial step. This section involves discretizing the computational domain into a finite number of grids. It takes a high-quality mesh to ensure simulation accuracy. In our work, we produce a hybrid mesh with hexahedral elements outside the building model and tetrahedral elements inside and close to the building.

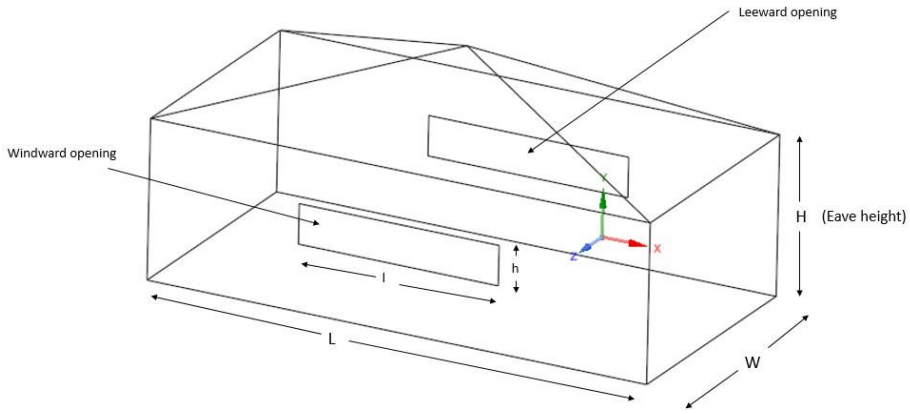

Fig 3.1: Three-dimensional view of the Pyramidal building

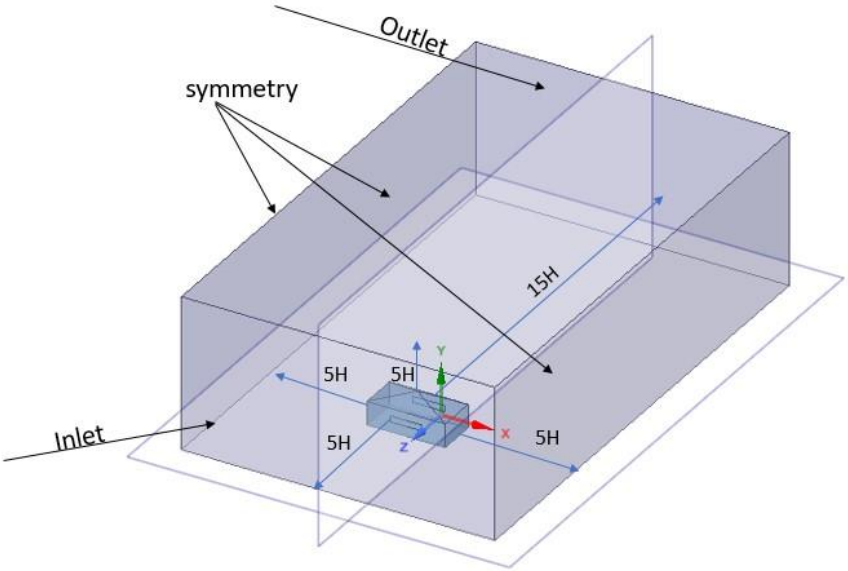

Fig 3.2: Three-dimensional view of computational domain

3.3 Governing Equation

Fluid flow motion is based on two fundamental equations: the Navier-Stokes equation and the continuity equation. Based on the idea of mass conservation, the continuity equation serves as the differential equation for the two equations mentioned above.

$$\frac{\partial u_i}{\partial x_i} = 0 \tag{3.1}$$

Navier -Stokes Equation (Derived from Newtons second law of motion)

$$u_j \frac{\partial u_i}{\partial x_j} = -\frac{1}{\rho}\frac{\partial p}{\partial x_i} + \frac{\partial}{\partial x_j}\left[v\left\{\frac{\partial u_i}{\partial x_j} + \frac{\partial u_j}{\partial x_i}\right\}\right] \tag{3.2}$$

Where, ui or uj = instantaneous velocity component along xi or xj direction

i = 1,2,3

j = 1,2,3

p = instantaneous pressure

v= kinematic viscosity of fluid = μ/ρ

μ= Dynamic viscosity of the fluid

ρ= Density of the fluid

3.4 Shear Stress Transport (SST) k-ω model

The k-ω turbulence model (SST) is an eddy-viscosity model with two equations. Mentor (1994) was the first to propose it [15]. This model combines two models: (i) the k-ε model and (ii) the ordinary k-ω model.

(i) The standard k-ω model: This model is perfect for modeling flow in the subviscous layer, which is the area close to the wall. The standard k-ω model is better suited for low Reynolds number flows since they are more sensitive, highly nonlinear, and difficult to converge.

(ii) k-ε model: For replicating flow that is flow little bit away from the wall, this model is perfect.

Consequently, this model is a hybrid that combines the advantages of the k-ω and k-ε models, switching between them based on the situation. Near the wall, the SST k-ω changes to k-ω after using the k-ε model in the free stream. In general, the SST k-ω model is less susceptible to free stream conditions, and it minimizes the accumulation of excessive turbulent kinetic energy at the stagnation point. Due to its ability to accurately predict flows with unfavorable pressure gradients and separation, the SST k-ω model is currently very popular. The model is made up of two transport equations that account for particular dissipation rate (ω) and turbulent kinetic energy (k).

The transport equations are as follows-

$$\frac{\partial}{\partial t}(\rho k) + \frac{\partial}{\partial x_i}(\rho k u_i) = \frac{\partial}{\partial x_j}\left(\Gamma_k \frac{\partial k}{\partial x_j}\right) + G_k - Y_k + S_k \quad (3.7)$$

$$\frac{\partial}{\partial t}(\rho \omega) + \frac{\partial}{\partial x_i}(\rho \omega u_i) = \frac{\partial}{\partial x_j}\left(\Gamma_\omega \frac{\partial \omega}{\partial x_j}\right) + G_\omega - Y_\omega + D_{\omega+} S_\omega \quad (3.8)$$

Where, ω = Specific dissipation rate

Gk = generation of turbulent kinetic energy due to mean velocity gradient

Gω = generation of specific dissipation rate

Γk = effective diffusivity of k

Γω = effective diffusivity of ω

Yk = the dissipation of k due to turbulence

Yω = the dissipation of ω due to turbulence

Dω = Cross diffusion term

Sk and Sω = user defined source terms

3.5 Boundary Conditions

The boundary conditions play an important role in the accuracy of the numerical solution of the governing equations. The appropriate boundary conditions selected will determine how accurate the numerical results are. The various boundary conditions employed in the current work to solve the governing equations are covered in the next section. The subsequent section addresses the various boundary conditions that were employed in the present investigation to solve the governing equations.

The following formula is used to calculate the streamwise velocity at the inlet

$$U(y) = \frac{u^*_{ABL}}{k}\, ln\left(\frac{y + y_0}{y_o}\right) \quad (3.9)$$

where k is the Von Karman constant (0.4), y is the height coordinate and aerodynamic roughness length (yo=0.0001 m), and u_ABL^* (=0.347 m/s)is the aerodynamic boundary layer (ABL) friction velocity, which is computed using the reference velocity (Uref =10 m/s) at eave height (yref=H=6m) [80].

Using equation (3.10), the turbulent kinetic energy can be computed.

$$k(y) = a(I_u(y) u(y))^2 \quad (3.10)$$

where the profile of streamwise turbulence intensity was chosen as $I_u(y) = \frac{1}{ln\left(\frac{y}{y_0}\right)}$ discovered in Karava (2008)[26], and the value of "a" was chosen as 1 (a=1), as advised by Tominaga et al. (2008)[81]. Equation (3.11) provides the turbulent dissipation rate.

$$\varepsilon(y) = \frac{u^{*3}_{ABL}}{k(y + y_0)} \quad (3.11)$$

The specific dissipation rate is defined in equation (3.12)

$$\omega(y) = \frac{\varepsilon(y)}{C_\mu k(y)} \quad (3.12)$$

Where the Cμ is an empherical constant taken as 0.09

The roughness constant Cs was taken to be 1 for the ground surface, and equation (3.13) could be used to calculate the sand grain roughness height ks based on their relationship with aerodynamic roughness length, yo.

$$k_s = \frac{9.793 y_0}{C_s} \quad (3.13)$$

Roughness height and roughness constant were considered to be 0 and 0.5 for building surfaces, respectively. The domain's output was subjected to zero static pressure. Furthermore, boundary conditions for symmetry are applied to the domain's top and two sides. A symmetry boundary condition occurs when the normal gradient of all the variables and the normal component of velocity are zero at the boundary.

3.6 Validation

The most important stage of CFD simulation is validation. This is done to find out how well the real situation can be numerically replicated by the CFD code. The outcomes of the CFD simulation are often contrasted with the available experimental data during validation. However, if experimental data is unavailable for a complex system, one or more representative subsystems that are simpler than the system as a whole may be used for validation.The current investigation's numerical findings were validated using the computational results of Karava et al. (2011)[27]'s experimental results.

3.6.1 Experimental setup

Particle Image Velocimetry (PIV) measurements were conducted in an open circuit Boundary Layer Wind Tunnel at Concordia University in Montreal by Karava et al. (2011)[27] to examine the cross-ventilation flow in cubic building models. Cast translucent polymethyl methacrylate (PMMA) sheets were used to create the building models, which were constructed at a 1:200 scale and measured (W x D x H) = (100 × 100 x 80) mm3. For this study, configurations of the opening were changed at three different heights on the windward walls, leeward walls and side walls say the top (h = 60 mm), middle (h = 40 mm), and bottom (h = 20 mm). This study examined the effects of varying wall porosity viz: 5%, 10%, and 20% on cross ventilation. The openings' width was only changed, and their height was maintained constant at 18 mm. In this case focus is on the opening height h=20mm (symmetric opening) with wall porosity 10%. Vertical profiles of mean wind speed and streamwise turbulence intensity were measured at the building position using a hot-film probe. At building height (H=80mm), a reference mean wind speed Uref = 6.97m/s and a streamwise turbulence intensity of 10% were observed; at ground level (12mm), the turbulence intensity was about 17%, and at gradient height (738mm), it was around 5%. For this investigation, an aerodynamic roughness length of z0=0.025mm (0.005m in full size) was taken into consideration.

3.6.2 Validation using CFD

The streamwise velocity is non dimensionalize with reference velocity and comparison of the streamwise and reference wind speed ratio (U/Uref) with the experimental results of Karava et al. (2011) [27] are done along a horizontal line that connects the midpoint of leeward opening and the windward opening respectively. A good agreement was seen between this result and the experiment result of karava et al (2011)[27] however the current CFD work showed minor deviation from the experimental work especially near the leeward opening which is due to the effect of shadow and reflection [44].

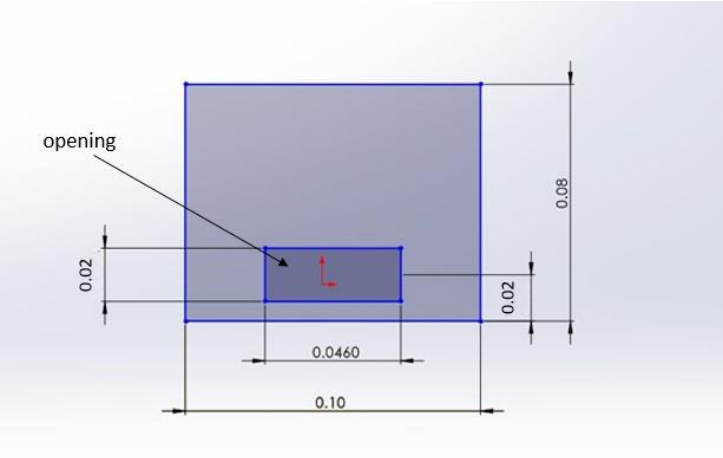

Fig 3.3: View of the model from inlet considered for validation as studied by Karava et al, (2011) [27]

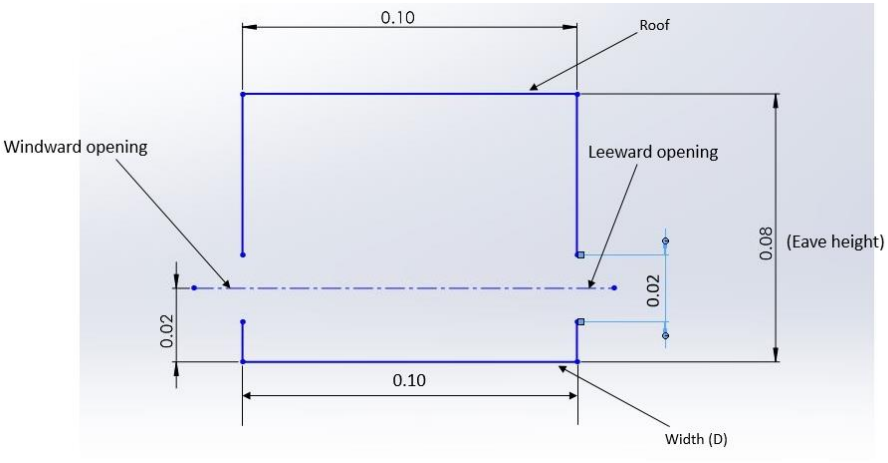

All dimensions are in metre (m)

Fig 3.4: Cross Sectional View of the model considered for validation as studied by Karava et al, (2011) [27]

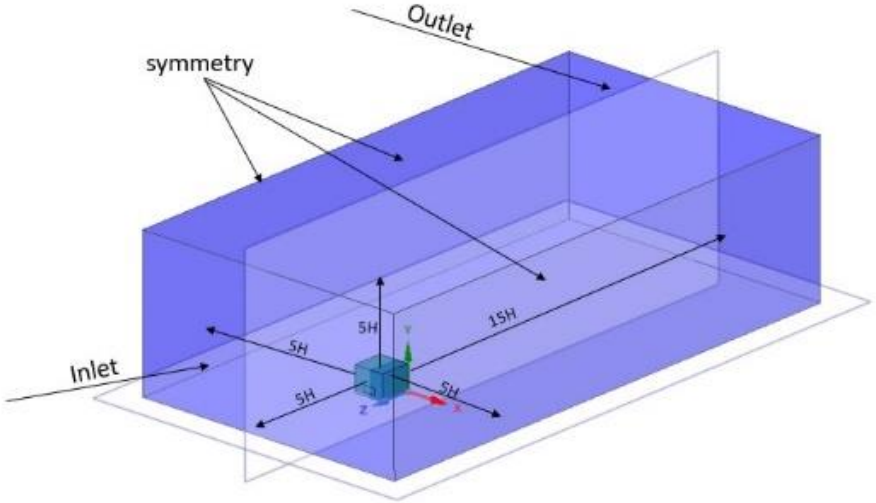

Fig 3.5: Computational Domain of the model considered for validation as studied by Karava et al, (2011) [27]

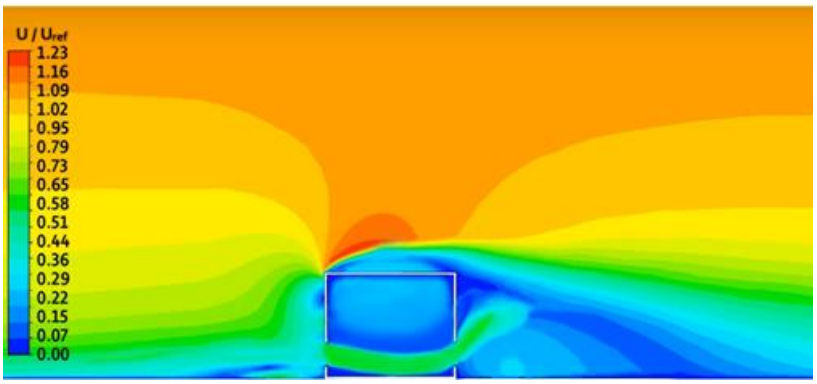

Fig 3.6: Non dimensional velocity contour U /Uref along the vertical mid plane.

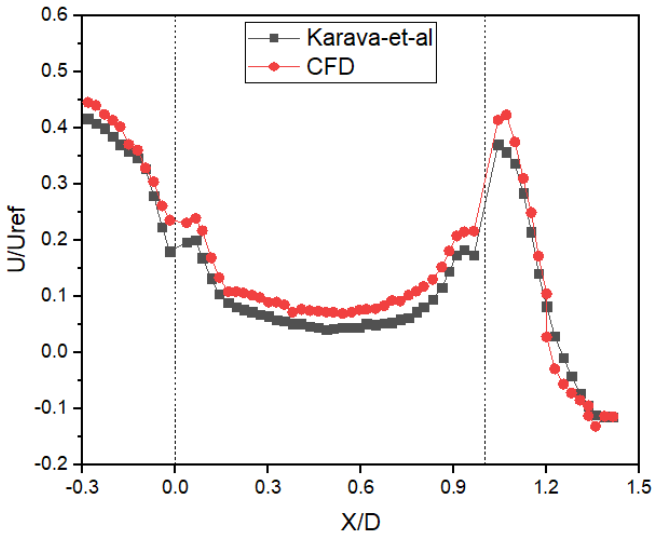

Fig 3.7: Non-dimensional streamwise wind velocity comparison at the centreline between the inlet and outlet openings.

3.7 Grid Independency test:

A grid sensitivity test must be conducted to get a suitable number of cell for accurate result with lesser computing time. In our case grid sensitivity test is done in a pyramidal building with symmetry opening. Since the opening is symmetry windward and leeward opening is at the same height from the ground which is 3 m and this case is refererred as the "Ref case". The dimension of the opening are 8m x 1.5 m as shown in fig 3.8. The roof pitch of the configuration is 6:10 i.e 3m from the eave height. The cross sectional view of the Pyramidal roof building is shown in Fig 3.9. In order to run the simulations, the velocity profile from equation (3.9) was taken into account, along with an aerodynamic boundary layer (ABL) friction velocity of 0.347 m/s for three distinct grids: a coarse grid with 1522223 cells, a basic grid with 2284012 cells, and a fine grid with 3425116 cells. For each of the three grids, the wind speed ratio (U/Uref) is obtained along the line connecting the midpoint of the windward and leeward openings and compared as shown in Fig.3.11. In the above three case a major difference between the result of coarse and basic grid is seen and a minor difference between the basic grid and fine grid is seen therefore basic grid with 2284012 cells is chosen for our case.

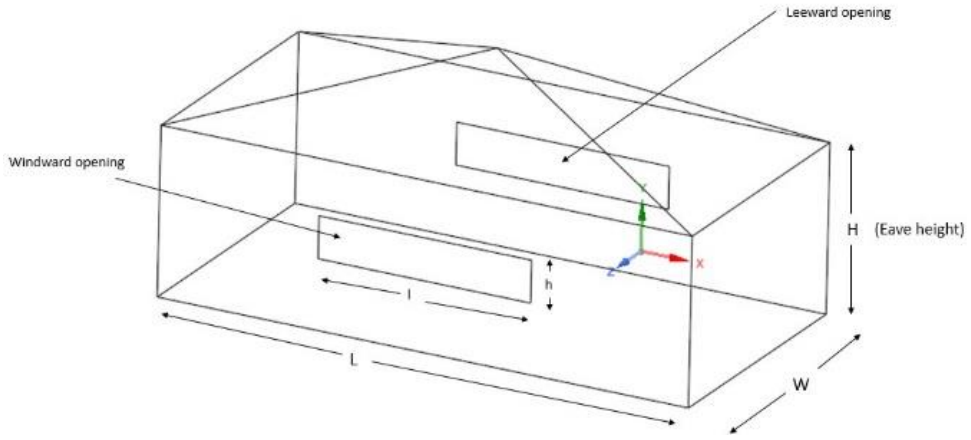

(All dimensions are in m)

Fig 3.8: Schematic diagram of Pyramidal building model with openings.

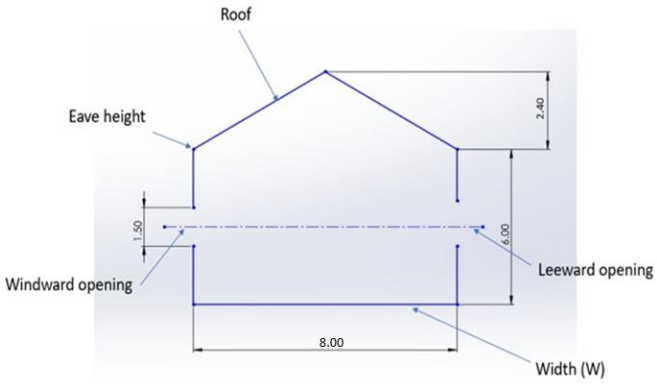

(All dimensions are in m)

Fig 3.9: Cross-sectional view of Pyramidal building (reference case)used for grid independency test

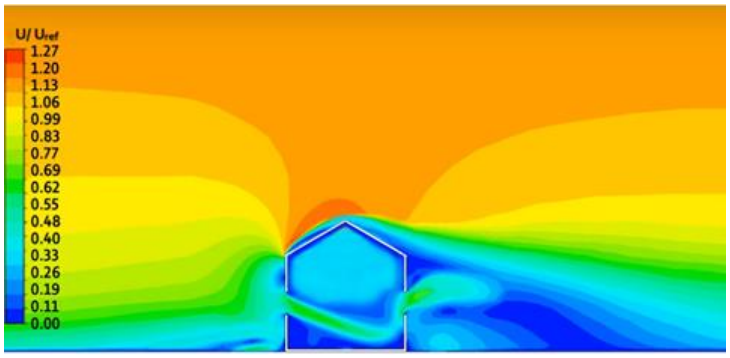

Fig 3.10: Non-dimensional velocity contour U /Uref along the vertical mid-plane for Basic grid

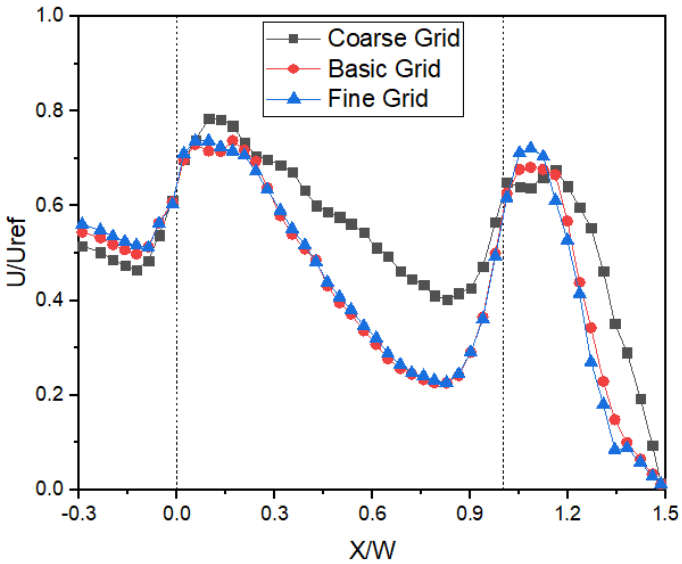

Fig 3.11: Grid indepedency test done by comparing non dimensional streamwise wind velocity ratio for different types of grid.

4.1 Defination of Problem

When examining wind flow around a structure with openings, the wall porosity is a crucial factor to consider. This is the reason this section focuses primarily on a thorough investigation of how wall porosity affects the flow field surrounding a Pyramidal roof rectangular base building. The four configurations listed in the earlier sections are taken into consideration for the numerical simulations, with different wall porosities for each configuration. The ratio of the opening area to the wall area is known as wall porosity.

$$\text{Wall porosity} = \frac{A_{opening}}{A_{wall}} \quad (4.1)$$

Aopening = Area of the opening (m2)
Awall = Area of the wall (m2)

The four wall porosities that were taken into consideration for each configuration in this study are 5%, 10%,15% and 20%, respectively. Table 4.1 provides the appropriate opening dimensions. Additionally, all layouts examined here have a roof pitch of 6:10, and only one wind incidence angle of 0^o i.e. when the direction of the wind incident is normal to the windward wall is taken. Figure 4.1 displays a schematic diagram of the building model with the size of the opening.

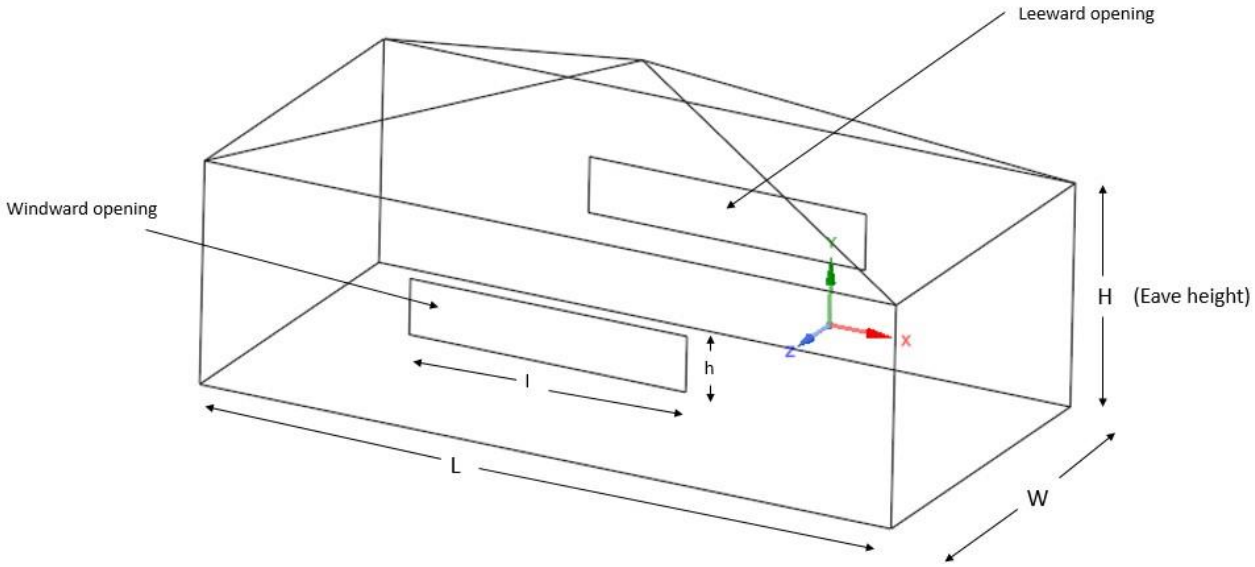

Figure 4.1: Schematic diagram of the building model with opening dimensions

Wall Porosity	Opening height (h) in metre	Opening width (l) in metre
5%	1.5	4
10%	1.5	8
15%	1.5	12
20%	1.5	16

Table 4.1: Opening dimensions and wall porosity.

4.2 Results and discussion

This section discusses the findings from the numerical simulations that were conducted to look at how different wall porosities affected the flow field. This section delivers three main results: (i) the velocity contour with different wall porosity, (ii) the mean internal pressure fluctuation with different wall porosity, and (iii)the non-dimensional air flow rate with different wall porosity.

4.2.1 The velocity contour with different wall porosity

To investigate the impact of wall porosity on the flow field, the velocity contour on the vertical mid-plane of the building model for each of the four configurations is taken into consideration. Figures 4.2 to 4.17 illustrate how the four distinct wall porosities in each configuration affect the variation in velocity vector field. The formation of the stream tube between the

windward and leeward apertures is one of the essential characteristics of the internal flow field. The stream tube becomes more apparent as wall porosity increases, which causes some major changes in the interior airflow pattern.

4.2.1(i). Velocity contour for configuration A

The stream tube bends upward as it enters the building and then changes direction downward before exiting through the leeward opening, as can be seen from the velocity vector field displayed in figure 4.2 to 4.5 for configuration A, where the windward opening is located above the mid-height and the leeward opening is located below the mid height. In this case, the stream tube expands in size as the wall porosity increases from 5% to 10% and some of the upward-moving air creates a small vortex above the stream tube. This vortex is more pronounced when the wall porosity reaches 15% and become blurred when wall porosity reaches 20%. A vortex below the outer side of windward section is distinct when the wall porosity increases from 5% to 10%, 15% and 20%. A vortex outside the leeward section start growing when wall porosity increases from 15% to 20%.

4.2.1(ii). Velocity contour for configuration B

The velocity vector field for configuration B, with the leeward opening above the mid-height and the windward opening below the mid-height, is shown in Figure 4.6 to 4.9. The stream tube is seen to descend as it passes through the windward opening and then to rise once again until it reaches the leeward opening but some of the air stream is seen to flow straight into the leeward aperture rather than moving downward, forming a little continuous stream tube between the two openings. This may be refer to as the short-circuiting effect [40]. This effect is prominent for wall porosity 15% and 20% which is due to the fact that increased wall porosity causes the airstream's size to increase.

4.2.1(iii). Velocity Contour for configuration C

A continuous stream tube forms between the windward and leeward openings in configuration C where the windward opening is above the mid-height and the leeward opening is just near the ground as shown in figure 4.10 to 4.13. On the other hand, as the wall porosity rises from 10% to 15% and 20% the stream tube gets larger as a result of it the airstream bends upward and a vortex forms just above the stream tube which is more distinct for 15% and 20% wall porosity. This causes a significant volume of air to accumulate inside the structure, which ultimately raises the internal pressure and increases the flow resistance.

4.2.1(iv). Velocity contour for configuration D

The velocity vector fields for configurations D is shown in Figures 4.14 to 4.17. In the above configurations, the windward opening is just above the ground while the leeward opening is above the mid-height. Since the air enters the structure from below here, it must shift its course upward in order to reach the outlet opening. As wall porosity increases and air enters through the bottom, the stream tube becomes more prominent as a result, more air is trapped close to the building ground surface. As a result, the flow encounters more resistance up to 15% wall porosity. As wall porosity increases from 15% to 20% some of the air stream is seen to flow straight into the leeward aperture rather than moving downward, forming a little continuous stream tube between the two openings which is due to the fact that increased wall porosity causes the airstream's size to increase. Moreover, vortex outside the windward side is seen absent in the entire configuration because air is entering the model just above the ground.

4.2.2 Mean internal pressure

Mean internal pressure is one of the important flow characteristics that is impacted by variations in wall porosity and indoor airflow distribution of the Pyramidal roof rectangular base building. The fluctuation of the mean internal pressure coefficient (Cpin) with wall porosity for four distinct building configurations is shown in Figures 4.18 to 4.21.

4.2.2(i) Mean internal pressure for Configuration A

Mean internal pressure is one of the important flow characteristics that is impacted by variations in wall porosity and indoor airflow distribution of the Pyramidal roof rectangular base building. The fluctuation of the mean internal pressure coefficient (Cpin) with wall porosity for four distinct building configurations is shown in Figures 4.18 to 4.21.

4.2.2(i) Mean internal pressure for Configuration A

Mean internal Pressure for configuration A, with different wall porosity is shown in figure 4.18. In configuration A where the leeward aperture is below the mid-height and the windward opening is above it, the internal pressure is found to increase as wall porosity increases up to 15% and found to decrease as wall porosity increases from 15% to 20%. This decrease is due to the blurring of vortex above the stream tube.

4.2.2(ii) Mean internal pressure for Configuration B

Mean internal Pressure for configuration B, with different wall porosity is shown in figure 4.19. For configuration B where the windward opening is below the mid height and leeward opening is above the mid height it is shown that when the wall porosity rises from 5% to 10%, the internal pressure rises However, when the wall porosity rises to 15%,and 20% the internal pressure decreases this may be due to the short circuiting effect [40].

4.2.2(iii) Mean internal pressure for Configuration C

Mean internal Pressure for configuration C, with different wall porosity is shown in figure 4.20. For configuration C where the windward opening is above the mid height and leeward opening is near the ground it is shown that when wall porosity

rises from 5% to 10%, there is minute decrease in internal pressure; but, when wall porosity rises from 10% to 15% and 20% there is a dramatic increase in internal pressure which is due to the vortex formation above the stream tube inside the Pyramidal roof rectangular base building.

4.2.2(iv) Mean internal pressure for Configuration D

Mean internal Pressure for configuration D, with different wall porosity is shown in figure 4.21. For configuration D where the windward opening is near the ground and leeward opening is above the mid height it is shown that the internal pressure is found to increase as wall porosity increases up to 15% and found to decrease as wall porosity increases from 15% to 20%. which may be due to the short-circuiting effect [40].

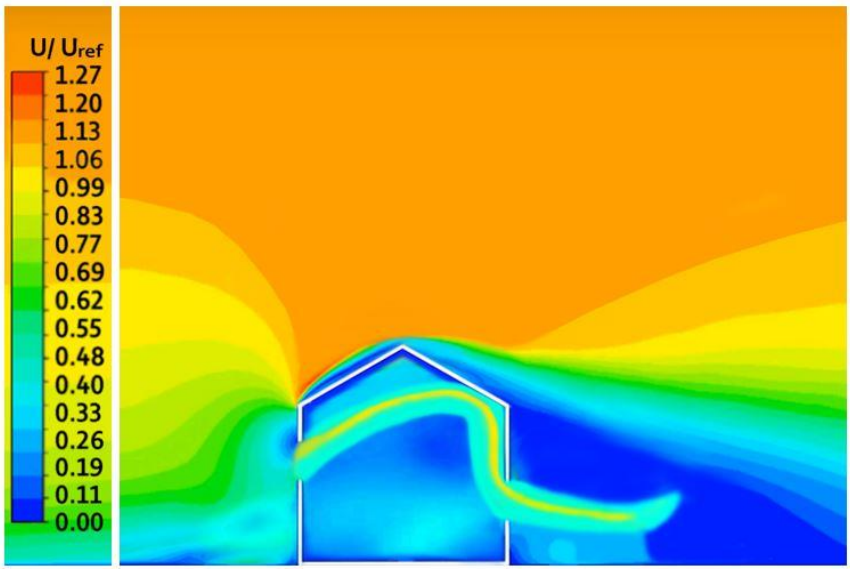

Fig 4.2: Velocity contour for configuration A with wall Porosity 5%.

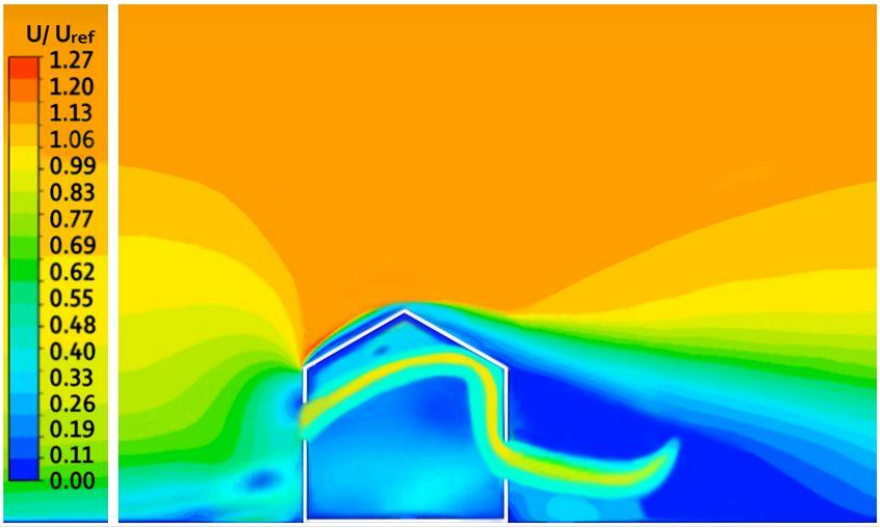

Fig 4.3: Velocity contour for configuration A with wall Porosity 10%.

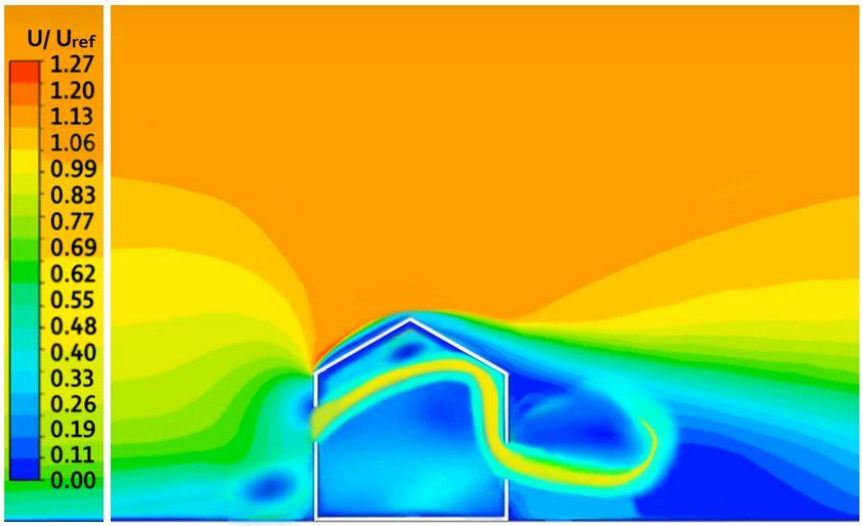

Fig 4.4: Velocity contour for configuration A with wall Porosity 15%.

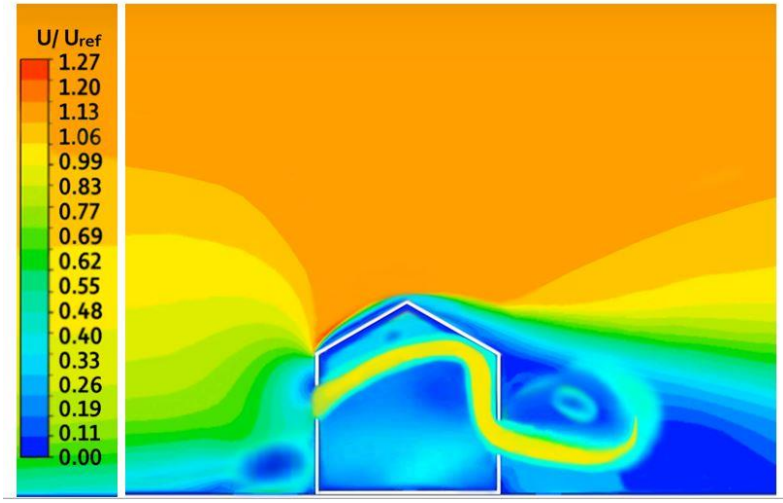

Fig 4.5: Velocity contour for configuration A with wall Porosity 20%.

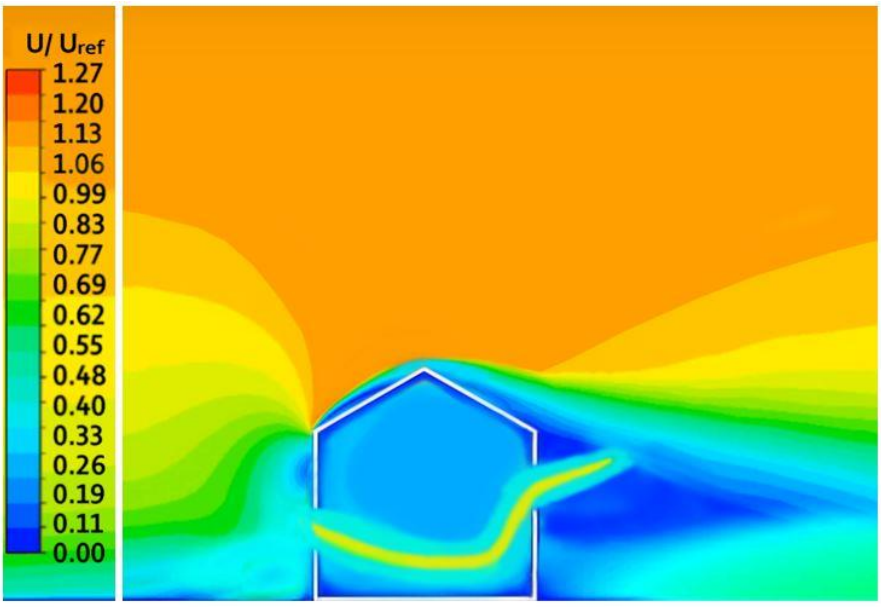

Fig 4.6: Velocity contour for configuration B with wall Porosity 5%.

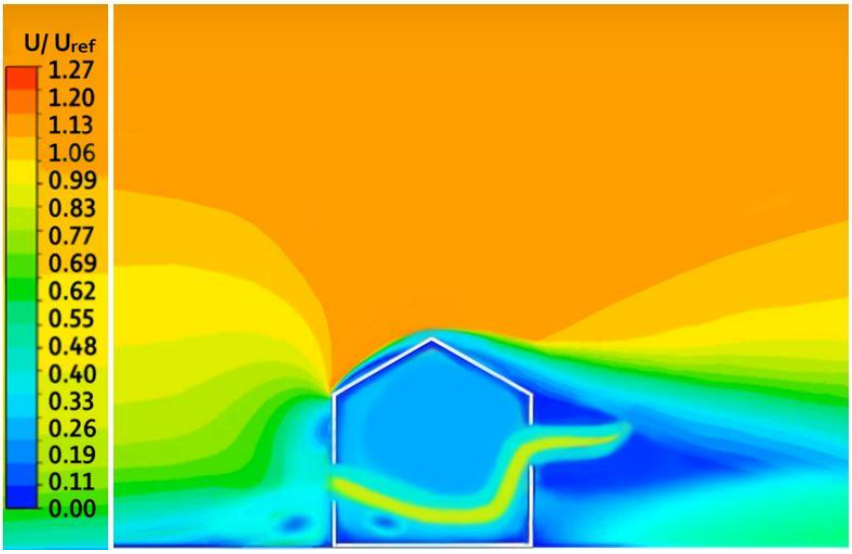

Fig 4.7: Velocity contour for configuration B with wall Porosity 10%.

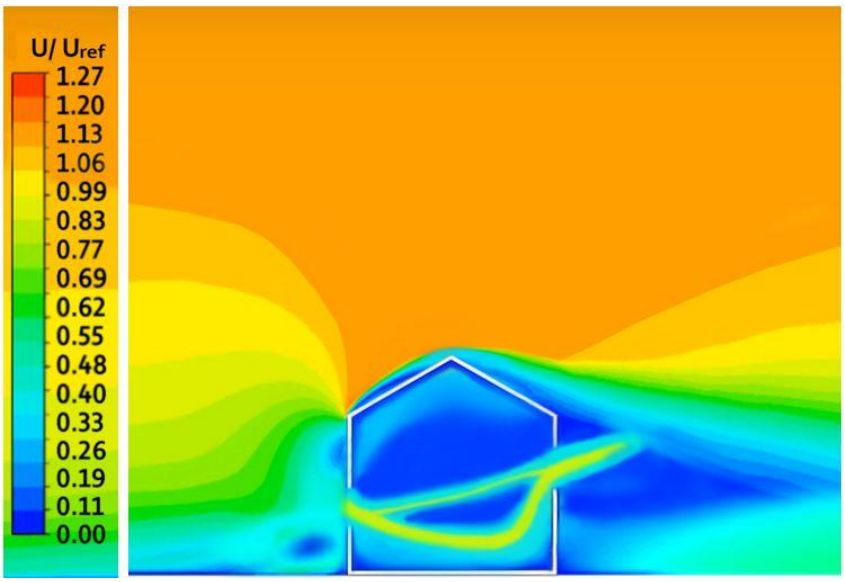

Fig 4.8: Velocity contour for configuration B with wall Porosity 15%.

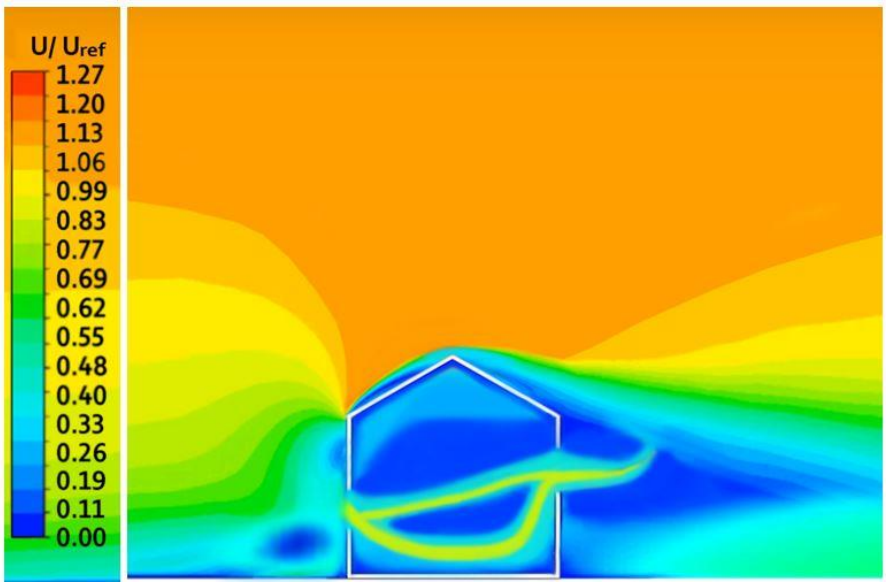

Fig 4.9: Velocity contour for configuration B with wall Porosity 20%.

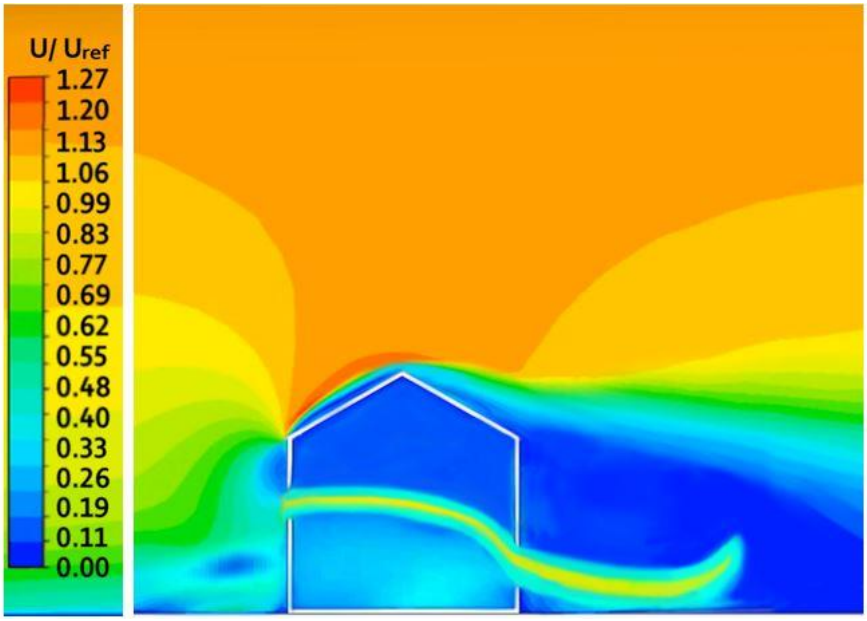

Fig 4.10: Velocity contour for configuration C with wall Porosity 5%.

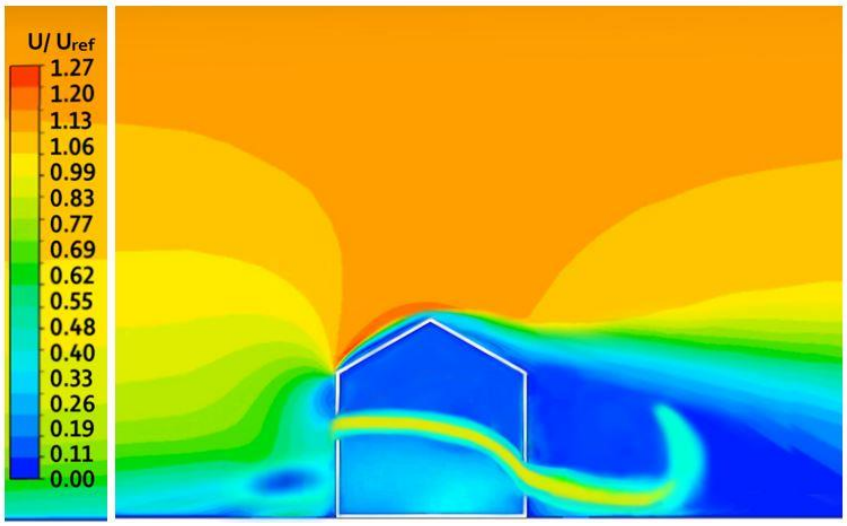

Fig 4.11: Velocity contour for configuration C with wall Porosity 10%.

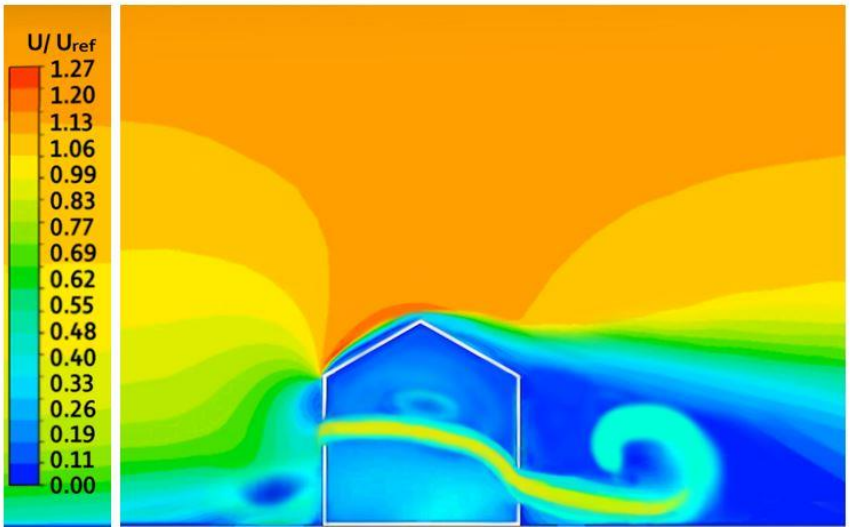

Fig 4.12: Velocity contour for configuration C with wall Porosity 15%

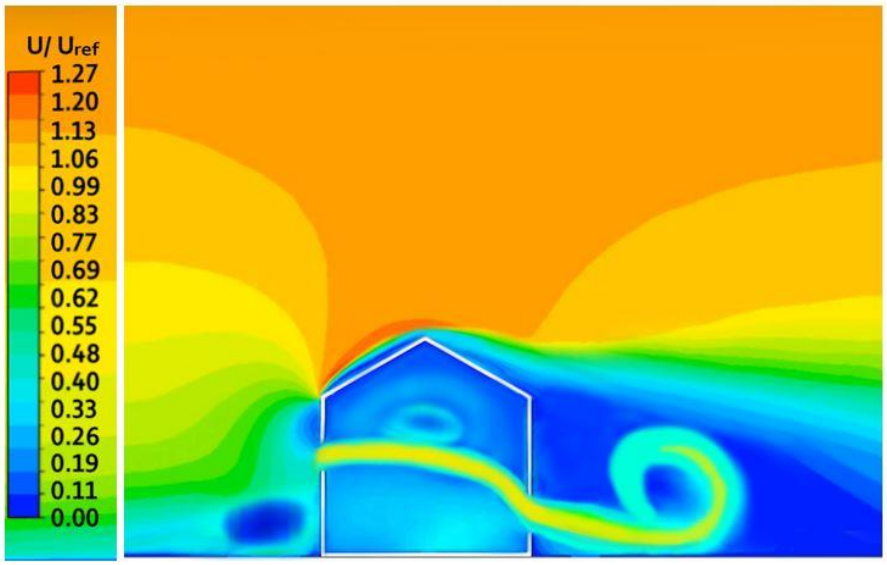

Fig 4.13: Velocity contour for configuration C with wall Porosity 20%.

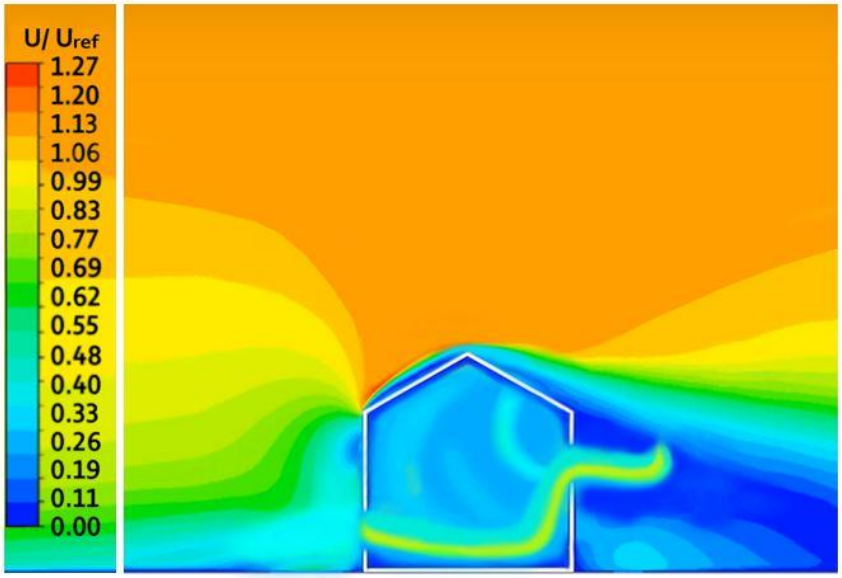

Fig 4.14: Velocity contour for configuration D with wall Porosity 5%.

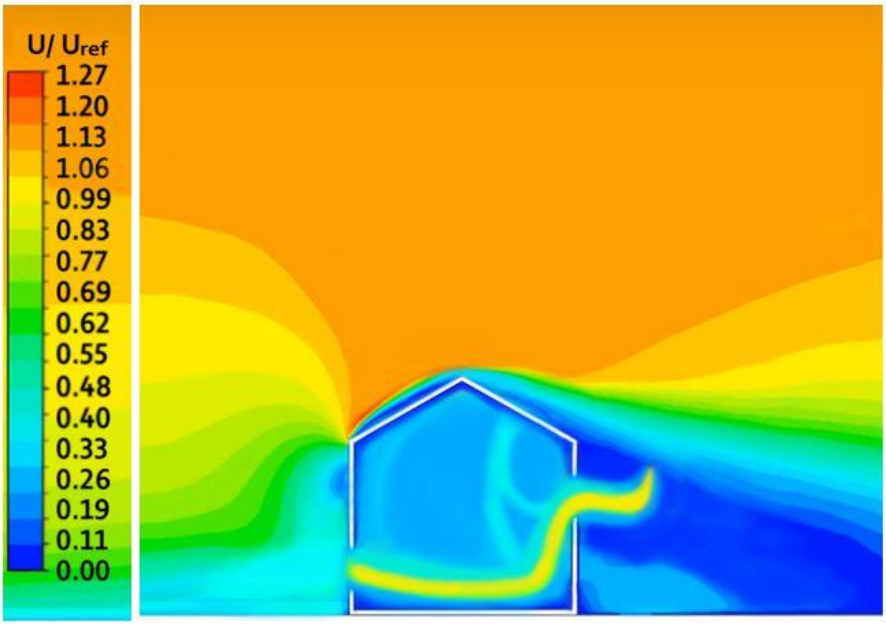

Fig 4.15: Velocity contour for configuration D with wall Porosity 10%.

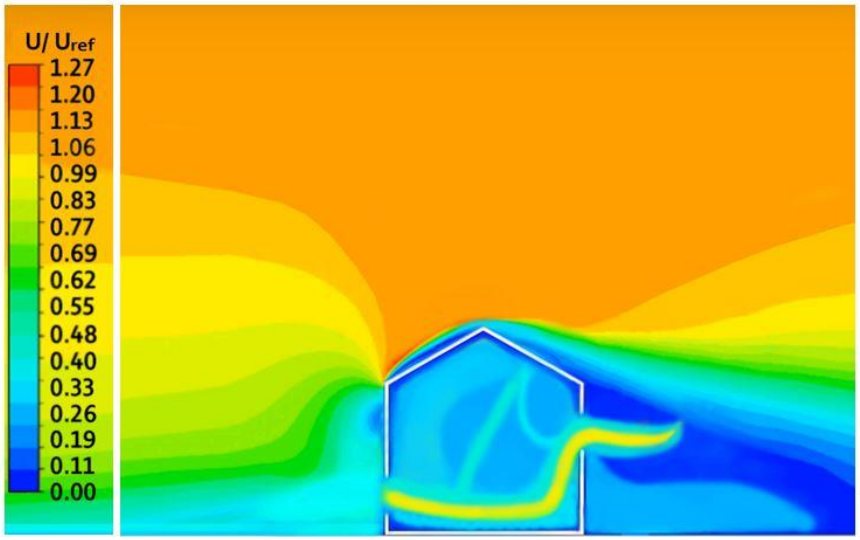

Fig 4.16: Velocity contour for configuration D with wall Porosity 15%.

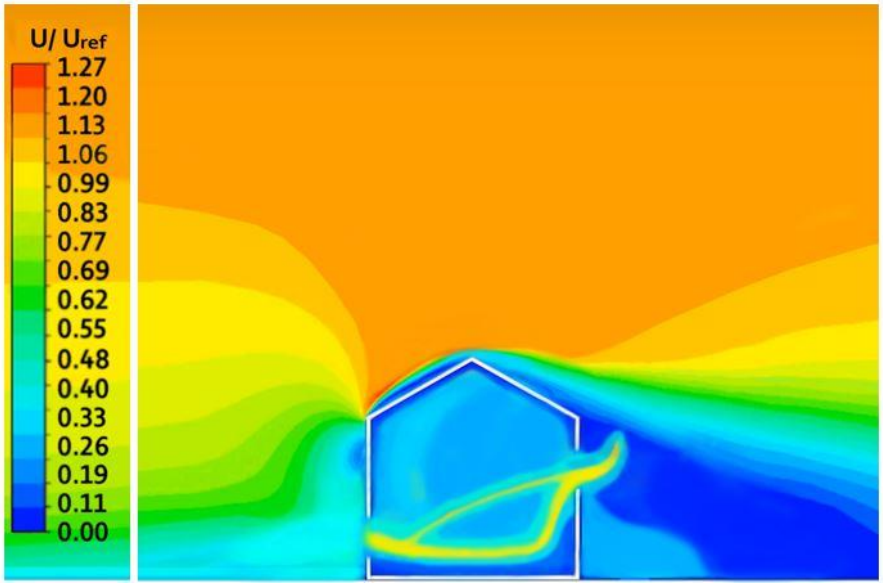

Fig 4.17: Velocity contour for configuration D with wall Porosity 20%.

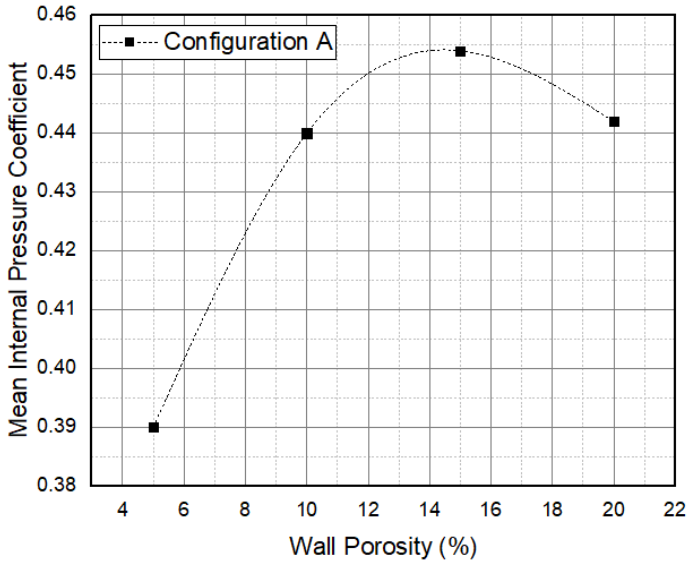

Fig 4.18: Variation of mean internal pressure coefficient with wall porosity for configuration-A

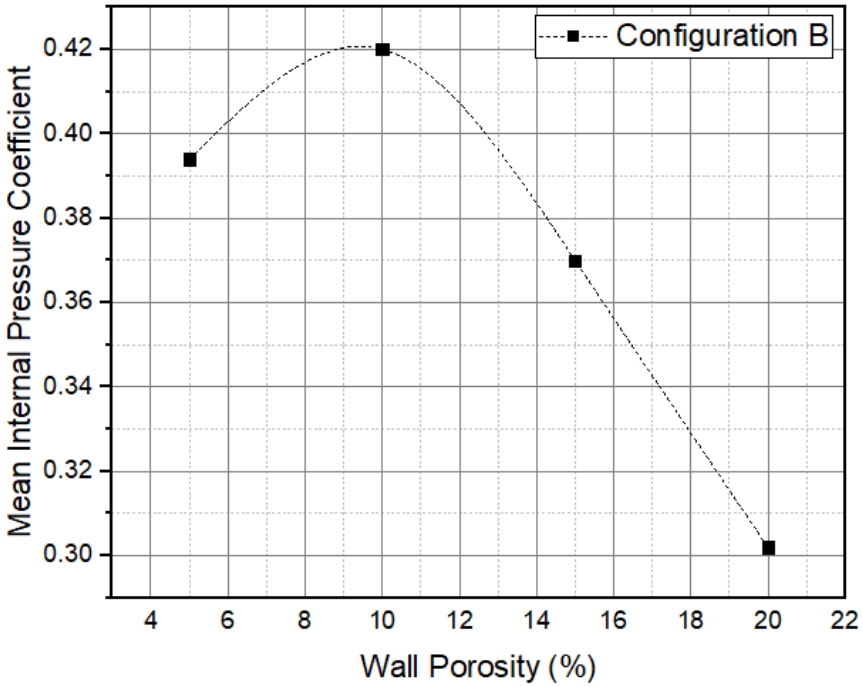

Fig 4.19: Variation of mean internal pressure coefficient with wall porosity for configuration –B

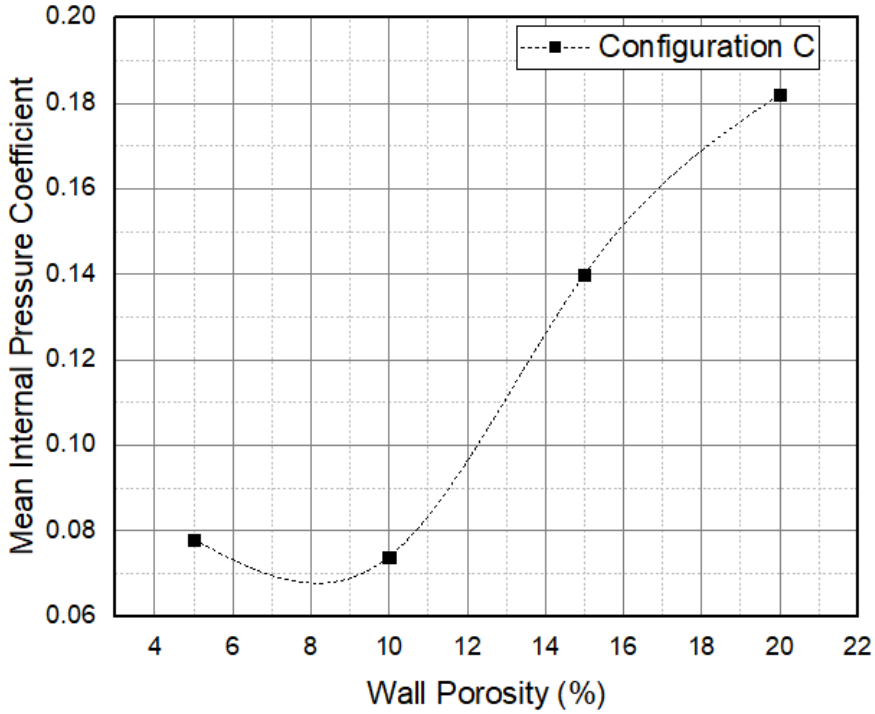

Fig 4.20: Variation of mean internal pressure coefficient with wall porosity for configuration –C

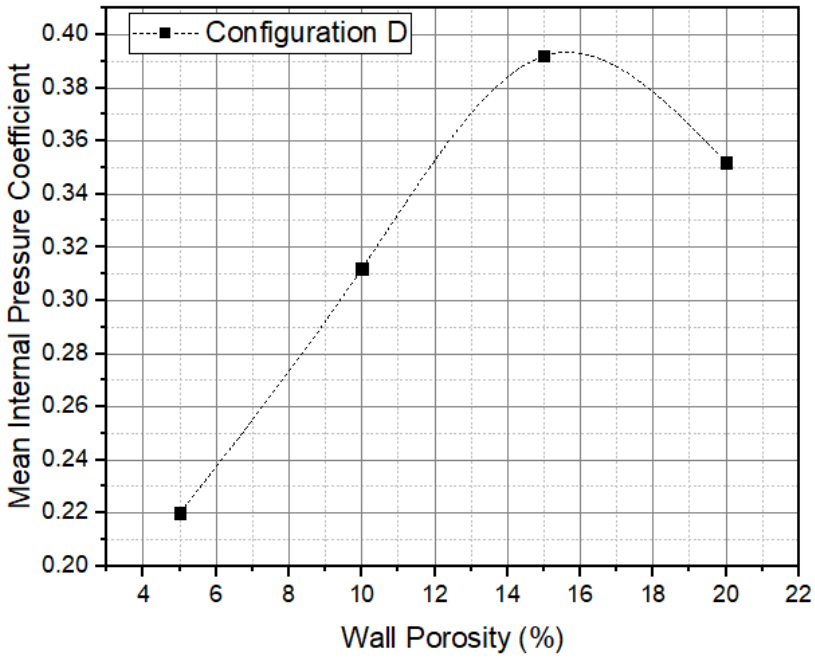

Fig 4.21: Variation of mean internal pressure coefficient with wall porosity for configuration –D

4.2.3 Air flow rate

Air flow rate is another one of the important flow characteristics that is impacted by variations in wall porosity and indoor airflow distribution of the Pyramidal roof rectangular base building. The influence of wall porosity on the interior flow field is investigated by estimating the airflow rate through the building model. Figures 4.22 to 4.25 show how the airflow rate varies with wall porosity. The wall porosity is shown on the x-axis, while the non-dimensional airflow rate is shown on the y-axis. The airflow rate is represented by a non-dimensional number known as the non-dimensional air flow rate, which is defined as

$$Q' = \frac{Q}{U_{ref}\, A_{op}} \qquad (4.2)$$

Q = Volume flow rate per sec (m3/sec)

Uref = Reference velocity at building eave height

Aop = Area of the opening

4.2.3(i) Air flow rate for configuration A

Air flow rate for configuration A decreases as the wall porosity increases from 5% to 10% and 15% which is due to the formation of vortex above the stream tube inside the building. The air flow rate again increases when wall porosity increases from 15% to 20% which may be due to the blurring of vortex above the stream tube inside the building and formation of vortex outside the leeward section of the Pyramidal roof rectangular base building.

4.2.3(ii) Air flow rate for configuration B

Air flow rate for configuration B decreases as the wall porosity increases from 5% to 10% which is due to the formation of vortex below the stream tube inside the windward side . The air flow rate increases sharply when wall porosity increases from 10% to 15% and 15% to 20% which may be due to the short circuiting of stream tube.

4.2.3(iii) Air flow rate for configuration C

Air flow rate for configuration C increases as the wall porosity increases from 5% to 10% because of increase in size of stream tube. However, there is a reduction in air flow rate when wall porosity increases to 15% and 20% which may be due to the formation of vortex above the stream tube inside the building.

4.2.3(iv) Air flow rate for configuration D

Air flow rate for configuration D decreases as the wall porosity increases from 5% to 10% and 15% which may be due to the trapping of air near the ground because of the increase in size of the stream tube. However, there is an increase in air flow rate when wall porosity increases to 20% which may be due to the formation of short circuiting of stream tube.

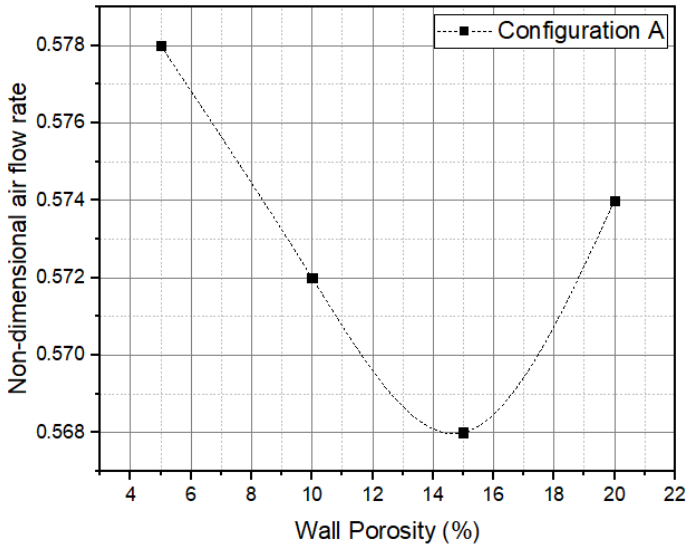

Fig 4.22: Variation of non-dimensional air flow rate with wall porosity for configuration-A

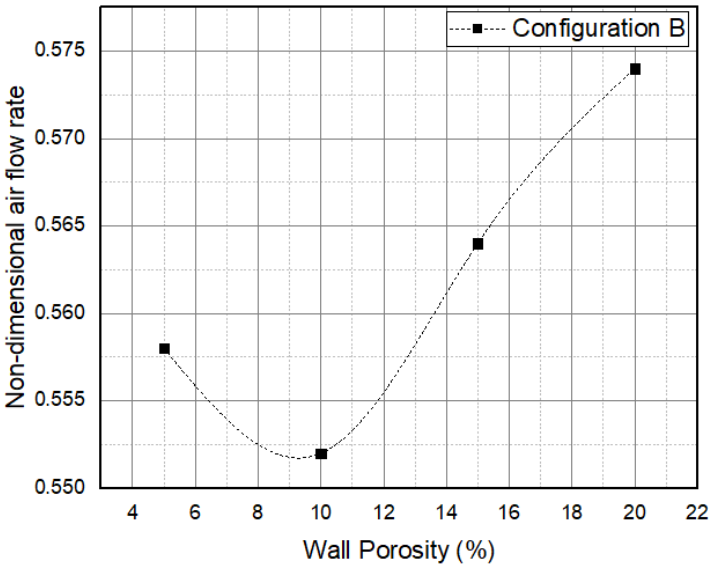

Fig 4.23: Variation of non-dimensional air flow rate with wall porosity for configuration-B

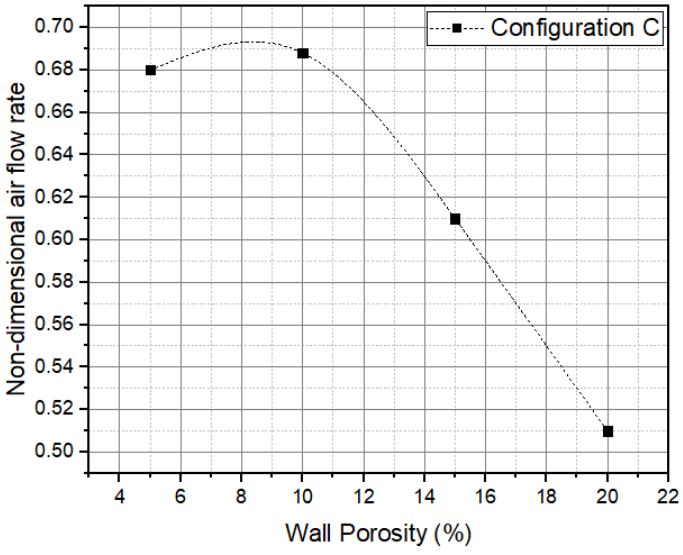

Fig 4.24: Variation of non-dimensional air flow rate with wall porosity for configuration-C

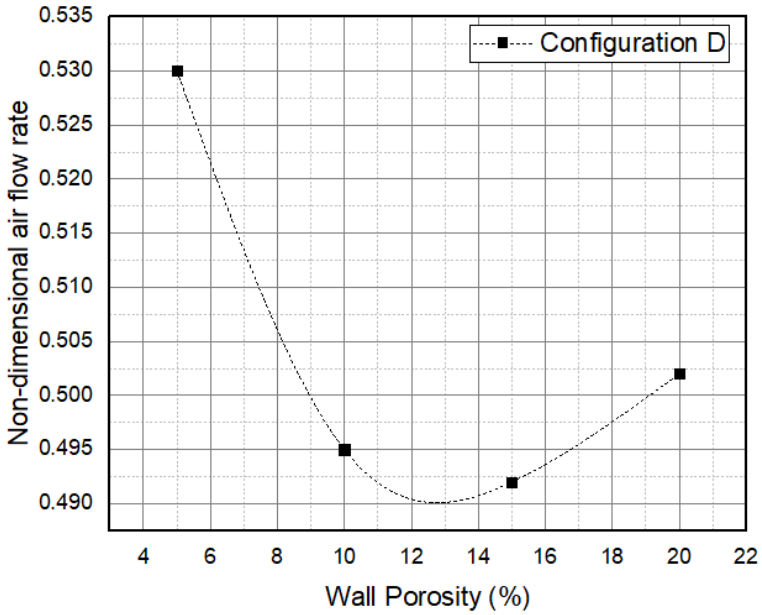

Fig 4.25: Variation of non-dimensional air flow rate with wall porosity for configuration-D

4.3 Conclusion

The current study examined the internal and external flow fields of Pyramidal roof rectangular base building structures with openings using numerical simulations. The numerical simulations were conducted using the commercially available CFD software ANSYS-FLUENT to examine the effects of vertical positions of the openings, wall porosity on the flow features inside and outside the building. The stable RANS equations are solved using the SST k-ω turbulence model. In the current study a significant impact of wall porosity is seen in the internal flow field.The internal flow field, which in turn influences the other internal flow parameters like air flow rate and mean internal pressure, is largely influenced by the wall porosity. The two most significant flow features of the internal flow field are the vortex creation and the short-circuiting effect. Flow field is also influenced by external flow parameters like flow separation, formation of vortex and blurring of vortex outside the leeward section of the Pyramidal roof rectangular base building.

Biblography

[1] J. P Cockroft and , P Robertson.: “Ventilation of an enclosure through a single opening”, Building and Environment, vol. 11(1), pp. 29–35,1976.

[2] Chu, Chia & Chiu, Y.-H & Tsai, Yi-Ting & Wu, Si-Lei. (2015). "Wind-driven natural 115 ventilation for buildings with two openings on the same external wall", Energy and Buildings, vol. 108, pp. 365–372, 2015.

[3] Dascalaki, M. Santamouris, A. Argiriou., C. Helmis, D.N. Asimakopoulos., K. Papadopoulos, A. Soilemes,,.: “On the combination of air velocity and flow measurements in single sided natural ventilation configurations”, Energy and Buildings, vol. 24(2), pp. 155–165, 1996.

[4] M. M Eftekhari, “Single-sided natural ventilation measurements”, Building Services Engineering Research and Technology, vol. 16(4), pp. 221–225,1995.

[5] J. D Ginger, and C. W Letchford,.: “Net pressures on a low-rise full-scale building” Journal of Wind Engineering and Industrial Aerodynamics, vol. 83(1–3), pp.,239–2501999.

[6] T. K Guha, R. N Sharma, and P. J Richards: "Influence factors for wind induced internal pressure in a low rise building with a dominant opening", vol.8(2), pp. 1–17, 2011.

[7] T. K Guha, R. N Sharma, and P. J Richards:"Internal pressure in a building with multiple dominant openings in a single wall: Comparison with the single opening situation", Journal of Wind Engineering and Industrial Aerodynamics, vol. 107–108, pp. 244–255, 2012.

[8] D. W Etheridge, and J. A Nolan, “Ventilation measurements at model scale in a turbulent flow”, Building and Environment, vol. 14(1), pp. 53–64, 1979.

[9] D.W Etheridge, “Unsteady flow effects due to fluctuating wind pressures in natural ventilation design - mean flow rates”, Building and Environment, vol.35 (2), pp. 111-133, 2000a.

[10] D.W Etheridge,.: “Unsteady flow effects due to fluctuating wind pressures in natural ventilation design - instantaneous flow rates”, Building and Environment, vol. 35 (4), pp. 321-337, 2000b.

[11] P Heiselberg, K Svidt and P. V Nielsen,“Characteristics of airflow from open windows”, Building and Environment, vol. 36(7), pp. 859–869,2001.

[12] Y Jiang, D Alexander, H Jenkins, R Arthur, and Q Chen,.: “Natural ventilation in buildings: Measurement in a wind tunnel and numerical simulation with large-eddy simulation”, Journal of Wind Engineering and Industrial Aerodynamics, vol. 91(3), pp. 331–353, 2003.

[13] S Kato, R Kono, T Hasama, R Ooka, and T Takahashi : "A wind tunnel experimental analysis of the ventilation characteristics of a room with singlesided opening in uniform flow", International Journal of Ventilation, vol. 5(1), pp. 171–178, 2006.

[14] P Heiselberg, K Svidt, and P. V Nielsen:“Characteristics of airflow from open windows”, Building and Environment, vol. 36(7), pp. 859–869,2001.

[15] M Sandberg: “An Alternative View on the Theory of Cross-Ventilation”, International Journal of Ventilation, vol. 2(4), pp. 409–418, 2004.

[16] M Sandberg, M Mattsson, H Wigö, A Hayati, L Claesson, E Linden,., M.A Khan: "Viewpoints on wind and air infiltration phenomena at buildings illustrated by field and model studies", Building and Environmen, vol. 92, pp.504–517, 2015.

[17] J Seifert, Y Li, J Axley, and M Rösler: "Calculation of wind-driven cross ventilation in buildings with large openings", Journal of Wind Engineering and Industrial Aerodynamics, vol. 94(12), pp. 925–947, 2006.

[18] S Murakami, S Kato, S Akabashi, K Mizutani,. and Y-D Kim: “Wind tunnel test on velocity-pressure field of cross-ventilation with open windows”, ASHRAE Transactions, vol. 97 (1), pp. 525-538, 1991.

[19] S Kato, S Murakami, A Mochida, S. Akabayashi, ichi, and Y Tominaga: “Velocity-pressure field of cross ventilation with open windows analyzed by wind tunnel and numerical simulation”, Journal of Wind Engineering and Industrial Aerodynamics, vol. 41-44, pp. 2575–2586, 1992.

[20] T Kurabuchi, M.Ohba, T Endo, Y Akamine, and F Nakayama: “Local dynamic similarity model of cross ventilation part 1 - theoretical framework”, International Journal of Ventilation, vol. 2 (4), pp. 371-382, 2004.

[21] M Ohba, T Kurabuchi, T Endo, Y Akamine, M Kamata and A Kurahashi, :“Local dynamic similarity model of cross ventilation part 2: application of Local dynamic similarity model”, International Journal of Ventilation, vol. 2 (4), pp. 383-393, 2004.

[22] K. R Gautam, L Rong, G Zhang, and M Abkar: "Comparison of analysis methods for wind-driven cross ventilation through large openings", Building and Environment, vol. 154, pp. 375–388, 2019.

[23] T. S Larsen,., and , P Heiselberg.: "Single-sided natural ventilation driven by wind pressure and temperature difference", Energy and Buildings, vol. 40(6), pp.1031–1040, 2008.

[24] P Karava, T Stathopoulos, and A. K Athienitis: “Wind driven flow through building openings”, Proceedings of International Conference on Passive and Low Energy Cooling for the Built Environment, pp. 427–432, Greece, 2005.

[25] R. N Meroney: "CFD Prediction of Airflow in Buildings for Natural Ventilation", Proceedings of 11th Americas Conference on Wind Engineering, pp. 1-11, San Juan, Puerto Rico, 2009.

[26] P Karava : Airflow Prediction in buildings for Natural Ventilation Design:wind tunnel measurements and simulation, Ph. D. Dissertation, Department of Building, Civil and Environmental Engineering, Concordia University, Montreal, Canada, 2008.

[27] P Karava, T Stathopoulos, and A. K Athienitis: "Airflow assessment in cross-ventilated, buildings with operable façade elements", Building and Environment, vol. 46(1), pp. 266–279, 2011.

[28] T Katayama, J Tsutsumi, and A Ishii: “Full-scale measurements and wind tunnel tests on cross-ventilation”, Journal of Wind Engineering and Industrial Aerodynamics, 41–44, 2553–2562, 1992.

[29] Y Iino, T Kurabuchi, N.Kobayashi, and A Arashiguchi: “Study on airflow characteristics in and around building induced by cross-ventilation using wind tunnel experiments and CFD simulation”, Sixth International Conference on Air Distribution in Rooms, Vol. 2, pp. 307–314, 1998.

[30] M Ohba, K Irie, and T Kurabuchi: “Study on airflow characteristics inside and outside a cross- ventilation model, and ventilation flow rates using wind tunnel experiments”, Journal of Wind Engineering and Industrial Aerodynamics, vol. 89, pp. 1513-1524, 2001.

[31] J. P. J True: Openings in Wind Driven Natural Ventilation. Ph.D. Thesis. Department of Building Technology and Structural Engineering, Aalborg University, Denmark, 2003.

[32] C. R Chu, and B. F Chiang: "Wind-driven cross ventilation in long buildings", Building and Environment, vol. 80, pp. 150–158, 2014.

[33] T van Hooff, B Blocken, and Y Tominaga: "On the accuracy of CFD simulations of cross-ventilation flows for a generic isolated building: Comparison of RANS, LES and experiments", Building and Environment, vol.114, pp. 148–165, 2017.

[34] M Manolesos, Z Gao, and D Bouris: "Experimental investigation of the atmospheric boundary layer flow past a building model with openings", Building and Environment, vol. 141(May), pp. 166–181, 2018.

[35] X Zhang, A. U Weerasuriya, and K. T Tse, "CFD Simulation of Natural Ventilation of a Generic Building in Various Incident Wind Directions: Comparison of Turbulence Modelling, Evaluation Methods, and Ventilation Mechanisms", Energy and Buildings, 110516, 2020.

[36] H Chiyoko, I Naoki, H Aya, and T Jun, "Computational fluid dynamics for cross-ventilated airflow in an urban building", Japan Architectural Review, in press, 2022.

[37] Z Tong, Y Chen, and A Malkawi, "Defining the Influence Region in neighborhood-scale CFD simulations for natural ventilation design", Applied Energy, vol. 182, pp. 625–633, 2016.

[38] M Bady, S Kato, T Takahashi, and H Huang, "Experimental investigations of the indoor natural ventilation for different building configurations and incidences", Building and Environment, vol. 46(1), pp. 65–74, 2011.

[39] M.Shirzadi, Y Tominaga, and P. A Mirzaei: "Wind tunnel experiments on cross-ventilation flow of a generic sheltered building in urban areas", Building and Environment, vol. 158, pp. 60–72, 2019.

[40] M Shirzadi, Y.Tominaga, and P. A Mirzaei: "Experimental study on cross ventilation of a generic building in highly-dense urban areas: Impact of planar area density and wind direction", Journal of Wind Engineering and Industrial Aerodynamics, 196 (November 2019), 104030, 2020.

[41] F Bazdidi-Tehrani, S Masoumi-Verki, and P Gholamalipour: "Impact of opening shape on airflow and pollutant dispersion in a wind-driven cross ventilated model building: Large eddy simulation", Sustainable Cities and Society, vol. 61, pp. 102196, 2020.

[42] Y Tominaga, and B Blocken, "Wind tunnel analysis of flow and dispersion in cross-ventilated isolated buildings: Impact of opening positions", Journal of Wind Engineering and Industrial Aerodynamics, vol. 155, pp. 74–88, 2016.

[43] Y Tominaga and B Blocken: "Wind tunnel experiments on cross-ventilation flow of a generic building with contaminant dispersion in unsheltered and sheltered conditions", Building and Environment, vol. 92, pp. 452–461, 2015.

[44] R Ramponi, and B Blocken: "CFD simulation of cross-ventilation flow for different isolated building configurations: Validation with wind tunnel measurements and analysis of physical and numerical diffusion effects", Journal of Wind Engineering and Industrial Aerodynamics, vol. 104–106, pp. 408–418, 2012.

[45] M Ohba, and I Lun: "Advances in Building Energy Overview of natural cross ventilation studies and the latest simulation design tools used in building ventilation-related", Advances in Building Energy Research, vol. 4(1), pp. 127–166, 2010.

[46] T Kobayashi, K Sagara, T Yamanaka, H Kotani, and M Sandberg: "Wind driven flow through openings - Analysis of the stream tube", International Journal of Ventilation, vol. 4(4), pp. 323–336, 2006.

[47] L. K Moey, Y. H Sing, V. C Tai, T. F Go and Y. Y Sia: "Effect Of Opening Size On Wind-Driven Cross Ventilation", International Journal of Integrated Engineering, vol. 13(6), pp. 99–108, 2021b.

[48] Y Hwang, and C Gorle: "Large-Eddy Simulations of Wind-Driven Cross Ventilation, Part1: Validation and Sensitivity Study", Frontiers in Built Environment, vol. 8, pp. 1–34, 2022.

[49] L. K Moey, K. L Chan, V. C Tai, T. F Go and P. L Chong: "Investigation on the effect of opening position across an isolated building for wind-driven cross ventilation", Journal of Mechanical Engineering and Sciences, vol. 15(2), pp. 8141–8152, 2021a.

[50] S Derakhshan, and A.Shaker: "Numerical study of the cross-ventilation of an isolated building with different opening aspect ratios and locations for various wind directions", International Journal of Ventilation, vol. 16(1). pp. 42-60,2016.

[51] N. F. M Kasim, S. A Zaki, M. S. M Ali, N Ikegaya, and A. A Razak: "Computational Study on the Influence of Different Opening Position on Windinduced Natural Ventilation in Urban Building of Cubical Array", Procedia Engineering, vol. 169, pp. 256–263, 2016.

[52] X Zhang, A. U Weerasuriya, J Wang, C. Y Li, Z Chen, K. T Tse, and J Hang: "Cross-ventilation of a generic building with various configurations of external and internal openings", Building and Environment, vol. 207(PA), pp. 108447, 2022.

[53] T Kobayashi, M Sandberg, T Fujita, E Lim, and N Umemiya: "Numerical analysis of wind-induced natural ventilation for an isolated cubic room with two openings under small mean wind pressure difference", Building and Environment, 226(September), 109694, 2022.

[54] S. F Díaz-Calderón, J. A Castillo, and G Huelsz: "Evaluation of different window heights and facade porosities in naturally cross-ventilated buildings: CFD validation", Journal of Wind Engineering and Industrial Aerodynamics, vol. 232(November 2022), pp. 105263, 2023.

[55] Y Tominaga and B Blocken: "Wind tunnel experiments on cross-ventilation flow of a generic building with contaminant dispersion in unsheltered and sheltered conditions", Building and Environment, vol. 92, pp. 452–461, 2015.

[56] B. J Vickery, R.E Baddour, and C. A Karakatsanis: Study of the external wind pressure distributions and induced internal ventilation flow in low-rise industrial and domestic structures, Technical Report No. BLWT-SS2-1983, United States, 1983.

[57] B. J Vickery and C. A Karakatsanis: “External wind pressure distributions and induced internal ventilation flow in low-rise industrial and domestic structures”, ASHRAE Transactions, vol. 93(2), pp. 2198- 2213, 1987.

[58] P Karava, T Stathopoulos. and A. K Athienitis: "Impact of Internal Pressure Coefficients on Wind-Driven Ventilation Analysis", International Journal of Ventilation, vol. 5:1, pp. 53-66, 2006.

[59] Q Yi, M König, D Janke, S Hempel, G Zhang, B Amon, and T Amon: "Wind tunnel investigations of sidewall opening effects on indoor airflows of a cross-ventilated dairy building", Energy and Buildings, vol. 175, pp. 163–172, 2018.

[60] A Mistriotis, G. P. A Bot, P Picuno, and G Scarascia-Mugnozza: “Analysis of the efficiency of greenhouse ventilation using computational fluid dynamics”; Agricultural and Forest Meteorology, vol. 85(3–4), pp. 217–228, 1997a.

[61] A Mistriotis, X Arcidiacono, P Picuno, G. P. A Bot, and G Scarascia- Mugnozza: “Computational analysis of ventilation in greenhouses at zeroand low-wind-speeds”, Agricultural and Forest Meteorology, vol. 88(1–4), pp. 121–135, 1997b.

[62] A Shklyar, and A Arbel : “Numerical model of the three-dimensional isothermal flow patterns and mass fluxes in a pitched-roof greenhouse”, Journal of Wind Engineering and Industrial Aerodynamics, vol. 92(12), pp. 1039–1059, 2004.

[63] T Norton, J.Grant, R Fallon, and D. W Sun.: "Assessing the ventilation effectiveness of naturally ventilated livestock buildings under wind dominated conditions using computational fluid dynamics", Biosystems Engineering, vol.103(1), pp. 78–99, 2009.

[64] T Norton, J.Grant, R Fallon and D. W Sun.: "Optimising the ventilation configuration of naturally ventilated livestock buildings for improved indoor environmental homogeneity", Building and Environment, vol. 45(4), pp. 983–995,2010.

[65] M. De Paepe, J. G Pieters, W. M Cornelis, D Gabriels, B Merci, and P Demeyer: "Airflow measurements in and around scale-model cattle barns in a wind tunnel : Effect of wind incidence angle", Biosystems Engineering, vol.115(2), pp.211–219, 2013.

[66] F Xing, D Mohotti, and K Chauhan: "Experimental and numerical study on mean pressure distributions around an isolated gable roof building with and without openings", Building and Environment, vol. 132, pp. 30–44. (2018a).

[67] R. N Sharma, and P. J Richards: “Net pressures on the roof of a low-rise building with wall openings”, Journal of Wind Engineering and Industrial Aerodynamics, vol. 93(4), pp.267–291, 2005.

[68] T Kobayashi, M Sandberg, H Kotani, and L Claesson: "Experimental investigation and CFD analysis of cross-ventilated flow through single room detached house model", Building and Environment, vol. 45(12), pp. 2723–2734,2010.

[69] A Hayati, M Mattsson, and M Sandberg: "A wind tunnel study of wind driven airing through open doors", International Journal of Ventilation, vol.18(2), pp. 113–135, 2018.

[70] M. K Esfeh, A Sohankar, A. R Shahsavari, M. R Rastan, M Ghodrat, and M Nili.:"Experimental and numerical evaluation of wind-driven natural ventilation of a curved roof for various wind angles", Building and Environment, vol. 205(August), pp.108275, 2021.

[71] J. I Perén, T van Hooff, B. C. C Leite, and B Blocken:"CFD analysis of cross-ventilation of a generic isolated building with asymmetric opening positions: Impact of roof angle and opening location", Building and Environment, vol. 85, pp. 263–276, 2015.

[72] J. I Perén, T van Hooff, B. C. C Leite, and B Blocken.:"CFD simulation of wind-driven upward cross ventilation and its enhancement in long buildings: Impact of single-span versus double-span leeward sawtooth roof and opening ratio", Building and Environment, vol. 96, pp. 142–156, 2016.

[73] J. Singh and A.K Roy:"CFD simulation of the wind field around pyramidal roofed single-story buildings. SN appl, Sci,1,1425 (2019).

[74] IS 875(Part3): “2015(2015) IS 875-3 Design loads(other than earthquake) for buildings and structures-code of practise.pdf,Bureau of Indian Standards,New Delhi”.

[75] E. Standard (2011) Eurocode 1: Actions on structures-Part1-4: “General actions-Wind actions. European Union”.

[76] S.A Keote, R Singh, & D Kumar(2015) :”Construction of Low Rise Buildings in Cyclone Prone Areas and Modification of Cyclone”. Journal of Energy and Power Sources. 2. 247-252.

[77] J Revuz, DM Hargreaves, JS Owen (2012) On the domain size for the steady-state CFD modelling of a tall building. Wind Struct15:313–329.

[78] JSingh & A. K. Roy (2019). Effects of roof slope and wind direction on wind pressure distribution on the roof of a square plan pyramidal low-rise building using CFD simulation. International Journal of Advanced Structural Engineering, 11(2), 231-254.

[79] Roy, A. K., Sardalia, A., & Singh, J. (2021). Wind Induced Pressure Variation on High-Rise Geometrically Modified Building Having Interference through CFD Simulation. Computational Engineering and Physical Modeling, 4(4), 26-38.

[80] D.M. Hargreaves and N.G Wright.: "The use of commercial CFD software to model the atmospheric boundary layer", The Fourth International Symposium on Computational Wind Engineering (CWE2006), Yokohama, 2006.

[81] Tominaga, Y., Mochida, A., Yoshie, R., Kataoka, H., Nozu, T., Yoshikawa, M.,and Shirasawa, T.: "AIJ guidelines for practical applications of CFD to pedestrian wind environment around buildings", Journal of Wind Engineering and Industrial Aerodynamics, vol. 96(10–11), pp. 1749–1761, 2008.

[82] Aly, Aly Mousaad & Khaled, Faiaz & Gol-Zaroudi, Hamzeh. (2020). Aerodynamics of Low-Rise Buildings: Challenges and Recent Advances in Experimental and Computational Methods. SN - 978-1-83880-167-0, DO - 10.5772/intechopen.92794.

[83] Ansys Fluent theory guide.